



THE

EARTH OBSERVER

A Bimonthly EOS Publication

May/June 2002, Vol. 14, No. 3

In this issue ...

FEATURED ARTICLES

Radiometric Measurement Comparisons
at NASA's Goddard Space Flight
Center: Part I. The GSFC Sphere
Sources 3

An Introductory Multidisciplinary Set
of MODIS Data for the Earth
Sciences Community 9

First Glimpses from Aqua 11

Using Landsat Data to Estimate Planted
Area and Production Levels of
Sugarcane in Argentina 12

An Overview of the Solar Radiation and
Climate Experiment 17

NEWS: Mixed Croplands May Make
Some Areas Cooler, Wetter in
Summer 23

REGULAR FEATURES

EOS Scientists in the News 24

Earth Science Education Program
Update 26

Science Calendars 27

The Earth Observer Information/
Inquiries Back Cover

EDITOR'S CORNER

Michael King

EOS Senior Project Scientist

I'm pleased to report that the successful launch of NASA's Aqua mission on May 4 has been followed by equally successful instrument activation and initial science data acquisition for all sensors. A final orbit-raising maneuver occurred on June 17, which raised Aqua to its operational altitude of 705 km. NASA Associate Administrator for Earth Science, Dr. Ghassem Asrar, released initial engineering imagery at the International Geoscience and Remote Sensing Symposium (IGARSS) in late June. The first science data from Aqua are scheduled to be released during a NASA press conference in September.

Aqua's orbit will continue to be adjusted to complement the equator crossing time of Terra, which crosses the equator at about 10:30 am. Aqua's final orbit will result in an equator crossing time of 1:30 pm, enabling diurnal observations of many parameters from the MODIS and CERES instruments, which are flown on both satellites.

Aqua will eventually fly in "formation" with other upcoming missions including CALIPSO, CloudSat, PARASOL, and Aura. Currently, Terra, Landsat 7, Earth Observing-1 (EO-1), and SAC-C missions are flying in formation. Coordinated orbits have the potential to multiply the observation capabilities of missions, enabling cross-correlation of data acquired and contributing to greater interdisciplinary Earth science research.

Other recently launched Earth observing missions continue to perform well, including the joint U.S./French Jason-1 ocean surface topography mission, the Stratospheric Aerosol and Gas Experiment (SAGE III), and the Gravity Recovery and Climate Experiment (GRACE). These missions are currently producing operational science data, and will undoubtedly result in new and

(Continued on page 2)

exciting research in the near future.

Comprehensive performance testing is nearing completion for the Solar Radiation and Climate Experiment (SORCE) mission, which is scheduled to launch on November 30 this year. SORCE measures the Sun's output with the use of state-of-the-art radiometers, spectrometers, photodiodes, detectors, and bolometers. Data obtained by the SORCE mission will be used to model the Sun's output and to explain and predict the effect of the Sun's radiation on the Earth's atmosphere and climate. A complete overview of the SORCE mission and the instruments flying onboard is presented on page 14 of this issue.

Additionally, the sole instrument on the upcoming Ice, Clouds and Land Elevation Satellite (ICESat) has been shipped to Ball Aerospace in Boulder, CO, for integration on the spacecraft. The Geoscience Laser Altimeter System (GLAS) is the first laser-ranging instrument designed for continuous global observations of the Earth and will accurately measure ice sheet mass balance, cloud and aerosol heights, and vegetation and land topography. ICESat is scheduled to launch in December of this year.

Together, these recent and upcoming missions will provide unprecedented Earth observation capabilities and lead to new and exciting insights in the Earth system. I look forward to bringing you updates on the progress of NASA's Earth Observing System in the coming months.

I am pleased to report that on June 18, 2002 the Earth Observatory <earthobservatory.nasa.gov> won the Webby People's Voice Award for



ODYSSEY OF THE MIND HOLDS WORLD FINALS IN COLORADO. *The 2002 Odyssey of the Mind World Finals were held at the University of Colorado at Boulder, May 22-25, 2002. The Opening Ceremonies brought together more than 12,000 people from 35 U.S. states and 14 countries to witness the lighting and spinning of the 16 ft internally lit MODIS globe produced by WorldFX, Cincinnati, OH, worldfx@earthlink.net.*

Science. It is an honor for this NASA Earth science site to be considered among the best Web sites in the world by the International Academy of Digital Arts and Sciences. Congratulations to everyone who contributes content to the site and many thanks to those of you who support it.

Lastly, the EOS Project Science Office was a prominent participant in the Odyssey of the Mind World Finals student competition May 22-26 in Boulder, Colorado. The photo above was taken during the opening ceremonies. This innovative and exciting competition attracts teams of students from all over the world, who apply ingenuity and creativity in solving technical problems posed by the organizers. This year, NASA sponsored a technical problem on the Earth's water cycle called "OMER's Earthly Adventures" after the raccoon-like Odyssey of the Mind mascot. This problem challenged students to correct a hypothetical environmental problem

using elements of technical innovation and theatrical performance. It is a creative exercise that combines science, education, and environmental responsibility in an instructional and innovative atmosphere. The top two winning teams in each Division were Georgia Tech, Atlanta, GA, and University of Kentucky, Lexington, KY, in Division 4; Amphitheater High School, Tucson, AZ, and No. 1 High School at East China University from Shanghai in Division 3; and William Penn Middle School, Yardley, PA, and Lower Dauphin Middle School, Hummelstown, PA, in Division 2. All of the teams performed a scientifically accurate and witty illusion of OMER traveling around the world preserving the environment.

It is a pleasure for NASA to be involved with Odyssey of the Mind, with both organizations representing the best of the best in innovation, teamwork, and creative problem solving.



Radiometric Measurement Comparisons at NASA's Goddard Space Flight Center: Part I. The GSFC Sphere Sources

- James J. Butler, butler@ltpmail.gsfc.nasa.gov, NASA's Goddard Space Flight Center
- B. Carol Johnson, cjohnson@nist.gov, National Institute of Standards and Technology
- Robert A. Barnes, rbarnes@seawifs.gsfc.nasa.gov, Science Applications International Corporation

Introduction

In 1995 the Earth Observing System (EOS) and the National Institute of Standards and Technology (NIST) formalized a comprehensive program to ensure the radiometric calibration accuracy of the sensors used in this global remote sensing program. A major component in the EOS calibration and validation program has been the deployment of NIST-traceable radiometers to EOS users' sites to assess the radiometric accuracy of source standards used to calibrate EOS sensors [1]. From March 26 through April 9, 2001, the National Aeronautics and Space Administration's Goddard Space Flight Center (NASA's GSFC) hosted such a comparison activity. The comparison took place in the GSFC Space Geodesy Networks and Sensor Calibration Office's (Code 920.1) Radiometric Calibration Facility (RCF) using its class 10,000 cleanroom facility (spectral.gsfc.nasa.gov). Radiometric sources other than those of the RCF were brought to the comparison for additional study. A total of thirteen radiometers from eight different groups were used to measure these sources. In this article, we summarize the preliminary results.

Sources Measured

During the comparison, a number of sources were measured. We present results from measurements of the RCF 182-cm diameter integrating sphere source (known as Hardy) and a 50.8-cm diameter integrating sphere from the Radiometric Calibration and Development Facility (RCDF) in the Atmospheric Chemistry and Dynamics Branch (Code 916) (designated the "Code 916" sphere). Hardy is used in the calibration of sun photometers that are part of a global network of *in situ* atmospheric characterization and in the calibration of other radiometers that are employed in the validation of EOS satellite instruments. The Code 916 sphere is used in the calibration of the Shuttle Ozone Limb Sounding Experiment/Limb Ozone Retrieval Experiment (SOLSE/LORE) and in the cross-calibration of the Optical Spectrograph and InfraRed Imaging System (OSIRIS), the Scanning Imaging Absorption spectrometer for Atmospheric Chartography (SCIAMACHY), and the Ozone Monitoring Instrument (OMI).

The sources were calibrated prior to the comparison, using the standard techniques of the associated group.

Hardy was calibrated over the spectral range from 400 nm to 2400 nm, using a single grating scanning monochromator (Optronics Laboratory model OL746 [2]) operating in the irradiance mode; this configuration is known as the 746/ISIC (Integrating Sphere Irradiance Collector) [3]. The Code 916 sphere was calibrated from 250 nm to 406 nm on April 1, 2001, using the Shuttle Solar Backscatter Ultraviolet (SSBUV) instrument as a transfer radiometer [4] and from 400 nm to 2400 nm on April 6, 2001 by the 746/ISIC. The uncertainties in the spectral radiance assignments depend on the methods used, the reference standards, and the wavelength ranges. The relative expanded uncertainties ($k = 2$) of the spectral radiances of Hardy and the Code 916 sphere, for example, are approximately 3.1% in the visible, increasing to 3.9% at 400 nm and 5.4% at 2400 nm. The spectral radiance uncertainty for the Code 916 sphere in the 300-nm to 400-nm ultraviolet wavelength range is 4.6% ($k = 2$), where k is defined as a *coverage factor* and corresponds to a 95.45% level of confidence.

Two additional sources were measured as well. To assess the accuracy of the responsivity scales of the transfer radiometers used in the measurement comparison, the participating radiometers measured the EOS/NIST Portable Radiance Source (NPR) [5]. Finally, to evaluate the implications of the recent improvements in the NIST spectral irradiance scale on remote-sensing uncertainties, two FEL lamp standards of spectral irradiance were used to illuminate a diffuse reflectance target. These results will be presented in Part II of this article.

Radiometers Used

The thirteen participating radiometers, their operating wavelengths, institutional affiliations, responsible personnel, and measurement uncertainties are provided in **Table 1**. The VXR, UAVNIR, UASWIR, UVFR, CTSS, LXR, and SXR-II are filter instruments; while the SWIXR, UVSR, SDSU ASD, GSFC ASD, 746/ISIC, and Ames ASD are grating instruments. The calibration of the radiometers varied depending on the team and the type of instrument.

The VXR, the UVFR, the UVSR, and the SWIXR, were calibrated using the NPR with all four lamps illuminated. The UAVNIR, UASWIR, 746/ISIC, Ames ASD, SDSU ASD, GSFC ASD, and the CTSS are all traceable to NIST, using lamp standards of spectral irradiance (1000 W FEL type lamps); for radiance calibration, these lamps illuminate diffuse reflectance standards. The SXR-II and the LXR were calibrated at NIST using a laser-based method that provides absolute

radiance responsivity within each channel [6].

Measurements

The primary goal of the comparison was to assess the uncertainties of (i.e., validate) the spectral radiance assignments to Hardy and the Code 916 spheres as implemented by their respective owners. A second objective was to examine the methods of operation for these sources and their temporal stability and repeatability.

TABLE 1: Radiometers Participating in the GSFC Radiometric Measurement Comparison

RADIOMETER	INSTITUTIONAL AFFILIATION	RESPONSIBLE PERSON	OPERATING WAVELENGTHS (nm)	MEASUREMENT UNCERTAINTY (k=1)
Visible Transfer Radiometer (VXR)	NIST/EOS	Carol Johnson	411.8, 441.0, 548.4, 661.4, 775.5, 870.0	1.2% @ 411.8 nm 0.7% @ 775.5 nm
Short-Wave Infrared Transfer Radiometer (SWIXR)	NIST/EOS	Steve Brown	800 to 2400	1.7%
Ultraviolet Scanning Radiometer (UVSR)	NIST	Ted Early	300 to 400	0.5%
Ultraviolet Filter Radiometer (UVFR)	NIST	David Allen	317.7, 325.1, 339.9, 388.0, 393.4	1.75%
U. of Arizona Visible/Near Infrared Radiometer (UAVNIR)	U. of Arizona	Stuart Biggar	412.8, 441.8, 488.0, 550.3, 666.5, 746.9, 868.1	2.1% @ 412.8 nm 2.2% @ 666.5 nm
U. of Arizona Short-Wave Infrared Radiometer (UASWIR)	U. of Arizona	Ed Zalewski	746.9, 868.7, 940.0, 1243.5, 1380.8, 1646.0, 2133.5, 2164.2, 2207.8, 2262.9, 2332.2, 2402.9	3.3% @ 900 nm 3.3% @ 1300 nm 3.3% @ 1600 nm 3.5% @ 2000 nm 3.9% @ 2400 nm
Landsat Transfer Radiometer (LXR)	NASA GSFC	Brian Markham Milton Hom Ed Kaita	480.7, 440.0, 560.7, 661.1, 662.3, 827.0	1.1% @ 440.0 nm 0.9% @ 662.3 nm
746 Integrating Sphere Irradiance Collector (746/ISIC)	NASA GSFC	John Cooper	400 to 2400	1.94% @ 400 nm 1.56% @ 1000 nm 2.22% @ 2200 nm
South Dakota State University Analytical Spectral Devices field radiometer (SDSU ASD)	South Dakota State University	Steven Schiller	350 to 2500	3% to 5%
GSFC Analytical Spectral Devices field radiometer (GSFC ASD)	NASA GSFC	Brian Markham Milton Hom Ed Kaita	350 to 2500	3% to 5%
SeaWiFS Transfer Radiometer II (SXR-II)	NASA GSFC	Gerhard Meister	410.7, 441.5, 487.6, 546.9, 661.9, 776.7	1.2% @ 410.7 nm 0.9% @ 776.7 nm
Calibration Transfer Standard Radiometer (CTSR)	Research Scientific Instruments	Don Heath	302.2, 305.6, 318.0, 321.6, 325.1, 339.7, 345.2, 437.5, 439.2, 525.0, 600.0, 674.6, 760.3, 923.3, 935.1	1.0%
Ames Analytical Spectral Devices field radiometer (Ames ASD)	NASA Ames	Pavel Hajek	350 to 2500	3% to 5%

The issue of sphere stability was tested using continuous monitoring with independent radiometers: a Filter Radiometer Monitoring System (FRMS) for Hardy [7] and the UVFR for the Code 916 sphere. In addition, the VXR was used twice in each measurement sequence, typically at the beginning and at the end. The repeatability of Hardy was investigated by repeating selected levels at different times.

Since the transfer radiometers have different center wavelengths and

bandwidths, the comparison of the radiance determined by the transfer radiometer to the radiance determined by the respective calibration facility was performed in the following manner. The spectral radiance assigned to the integrating sphere using the calibration method, $L(\lambda)$, was interpolated to intervals of 0.1 nm, as were the individual relative spectral responsivities, $r(\lambda)$, (or slit scattering functions in the case of the grating instruments). For each measurement

wavelength, these two functions were multiplied and summed over all wavelengths to determine the predicted band-averaged spectral radiance, L_p :

$$L_p = \frac{\int r(\lambda)L(\lambda)d\lambda}{\int r(\lambda)d\lambda}$$

Then, the band-averaged spectral radiance measured by the radiometer, L_m , was compared to L_p .

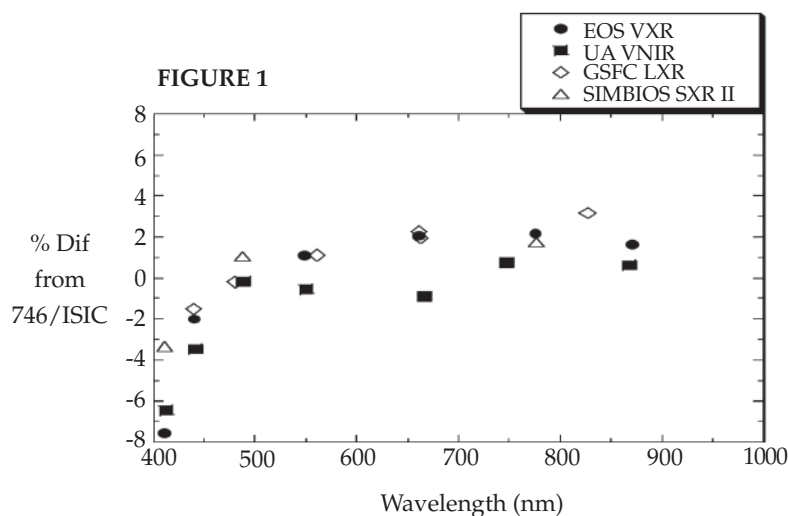


FIGURE 1 shows preliminary results for the 16-lamp Hardy sphere measurements in the visible/near-infrared compared to the GSFC 746/ISIC measured radiances.

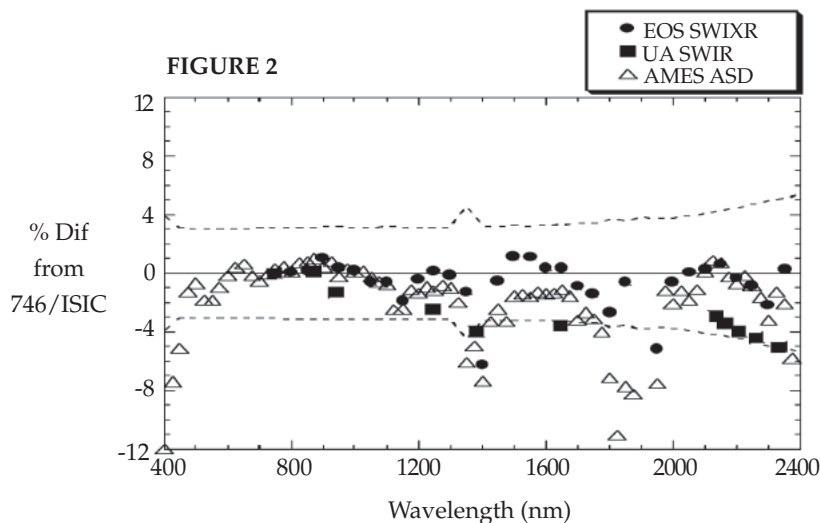


FIGURE 2 shows preliminary results for the 16-lamp Hardy sphere measurements in the shortwave infrared compared to the GSFC 746/ISIC measured radiances. The dashed lines indicate the $k = 2$ calibration uncertainty of the source using the 746/ISIC.

Results for Hardy Sphere

The spectral radiance scale assigned to the Hardy sphere by the 746/ISIC instrument was investigated at the 16- and 6-lamp illumination levels by the VXR and SWIXR, the UAVNIR and UASWIR, the LXR, the SXR-II, and the Ames ASD. The preliminary comparison results for the 16-lamp level are shown in **Figures 1 and 2**, divided by spectral range. The results are shown as $((L_m - L_p) / L_p) \times 100\%$, where L_m is the radiometer measured radiance and L_p is the radiance predicted from the 746/ISIC calibration. In cases where the radiometer made repeat measurements (i.e., the VXR and Ames ASD), the average results are used.

The preliminary results on the Hardy sphere show that neither the 16- nor the 6-lamp level was stable for wavelengths below 550 nm, with the sphere radiance increasing between 1-2% in the 411.8-nm channel in the time between subsequent VXR measurements on the same day (i.e., between 3

hours and 5 hours elapsed time). This result was supported by the measurements of the FRMS, which detected a 1% increase in sphere radiance at 411 nm during this time. The 6-lamp level was also not repeatable at the shorter measurement wavelengths on the two measurement days. The largest discrepancy observed with the VXR was 2.8% at 411.8 nm.

Results for Code 916 Sphere

The UV spectral radiance scale assigned to the Code 916 sphere by the Shuttle Solar Backscatter UltraViolet (SSBUV) instrument was investigated at the 4-lamp illumination level by the UVFR and UVSR. The SSBUV instrument, which resides solely in the RCDF cleanroom, is the flight model of the shuttle instrument which validated the ozone measurements of the Total Ozone Mapping Spectrometer (TOMS) and the Solar Backscatter UltraViolet (SBUV) instruments in the 1980s and early 1990s. Because of its wavelength

coverage, the RSI CTSS can be compared to both radiance assignments. The results are shown in **Figure 3**

The UVFR measured the Code 916 sphere at the beginning and end of the measurement day on April 3 and April 4. Based on these measurements, the sphere is very stable with a maximum difference of 0.5% at 317.7 nm. When the UVFR was not measuring in a position normal to the sphere aperture, it was also used as an off-axis stability monitor at 388.0 nm. At that wavelength, the UVFR detected a maximum change of 0.55% in the sphere output over approximately 7 hours of continuous operation. In addition to the UVFR, the VXR also measured the Code 916 twice on April 3 and twice on April 4, albeit in the visible and near infrared wavelength ranges. The VXR results supported the UVFR results, predicting the sphere to be very stable with a maximum difference of 0.5% at the wavelength closest to the ultraviolet, 411.8 nm.

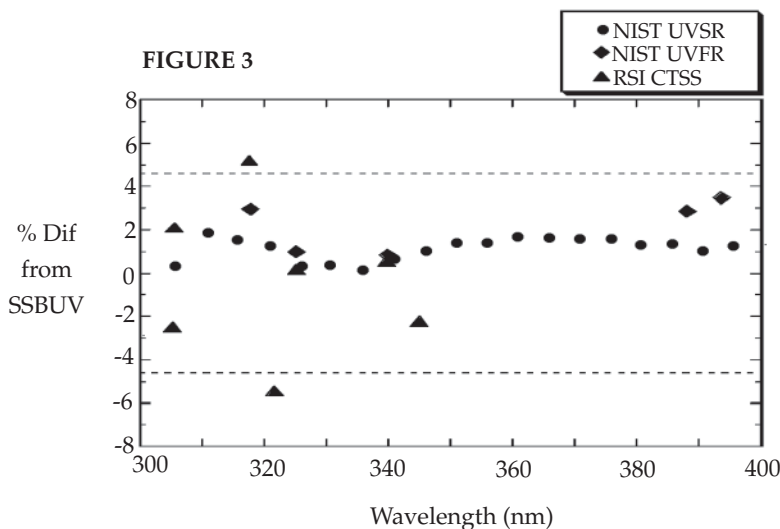


FIGURE 3 shows preliminary results for the Code 916 sphere measurements in the ultraviolet compared to the SSBUV measured radiances. The dashed lines indicate the $k = 2$ calibration uncertainty of the source using the SSBUV instrument.

Discussion

The results are judged by the combined expanded uncertainties of the measurement, which includes the source and the radiometer. We use a coverage factor, k , equal to 2, which corresponds to a 95.45% level of confidence. As a reminder, the EOS program requires accurate measurements: typically 3% to 5% ($k=1$) for radiance or irradiance in the UV, visible, and SWIR, with long-term stability requirements of better than 1%.

The results for Hardy in the visible and near infrared, shown in **Figure 1**, are reasonable over much of this range. However, the 746/ISIC results are higher than expected in the spectral region below about 450 nm. Possible sources for this discrepancy related to the 746/ISIC include: 1) spectral stray light effects due to the spectral shape of the standard irradiance lamp (i.e., F512) used to calibrate the 746/ISIC differing from that of Hardy coupled with the 746/ISIC being a single grating instrument; 2) non-linearity between the high gain ranges of the 746/ISIC; and 3) scattered light in the room being difficult to control in an instrument with a cosine collector. The measured temporal drift of Hardy or its spatial radiance uniformity could also contribute to the discrepancy.

The preliminary results for Hardy in the SWIR, **Figure 2**, are within the combined expanded uncertainties. Of course, the results in the water vapor absorption regions, near 1380 nm and 1850 nm, cannot be considered because of the natural variability in the amount of water vapor. The Ames ASD results

are particularly encouraging because it is an improvement, by almost a factor of two, in previous comparisons to the 746/ISIC using the NPR, indicating that the comparison with NASA Ames has indeed resulted in improved measurements [8].

In the UV, see **Figure 3**, the agreement between the UVSR and the UVFR with the SSBUV-derived scale for the Code 916 sphere is within the expanded $k=2$ uncertainties. The CTSS results have greater scatter, and two CTSS points are outside the $k=2$ calibration uncertainty of the sphere. However, all CTSS data are within the combined expanded uncertainties of the Code 916 sphere calibration and the CTSS measurements (see **Table 1**).

Summary

The radiometric measurement comparison held in GSFC's RCF in March and April 2001 involved 13 radiometers and was the largest EOS comparison to date. The transfer radiometers successfully validated the GSFC assigned radiance scales for Hardy and the Code 916 spheres. We observed that the Hardy sphere is not temporally stable when compared to other spheres such as the Code 916 sphere. However, the comparison established that the new monitoring system for Hardy, the FRMS, is an accurate indicator of the Hardy spectral radiance, and correction protocols for the temporal drift of the Hardy radiance using the FRMS are currently being investigated. The Code 916 sphere performed well, demonstrating excellent stability and repeatability. The improved agreement (compared to Hardy) at 412 nm and

441 nm between the core transfer radiometers and the 746/ISIC is of interest, because the accuracy of Hardy in this spectral interval is important for sun photometer and sky radiometer calibrations [9].

It is gratifying to observe the agreement between the NASA Ames ASD and the NASA GSFC 746/ISIC for measurements of Hardy because these radiometers are used to assign radiance scales to integrating spheres used in the calibration of a number of airborne and ground-based validation instruments, and previous results had been unsatisfactory.

Finally, the conditions for measurement in this activity were optimal: constant temperature and humidity, no dust, and no battery operation. The performance of field radiometers such as the SDSU ASD and the CTSS under actual measurement conditions could result in larger uncertainties than demonstrated in this work.

List of Participants

Jim Butler and **Brian Markham**, NASA's Goddard Space Flight Center; **Carol Johnson**, **Steve Brown**, **Ted Early**, and **David Allen**, NIST; **Stuart Biggar** and **Ed Zalewski**, University of Arizona's Remote Sensing Group; **Milton Hom** and **Ed Kaita**, Science Systems and Applications Incorporated; **John Cooper**, **John Marketon**, and **Gilbert Smith**, Raytheon Information Technology and Scientific Services; **Gerhard Meister**, Futuretech Corporation; **Pavel Hajek** and **Bob Barnes**, Science Applications International Corporation; **Stephen Schiller**, South

Dakota State University; and **Don Heath**, Research Scientific Instruments.

References

[1] Butler, J.J., B.L. Markham, B.C. Johnson, S.W. Brown, H.W. Yoon, R.A. Barnes, S.F. Biggar, E.F. Zalewski, P.R. Spyak, F. Sakuma, and J.W. Cooper, 1999: Radiometric measurement comparisons using transfer radiometers in support of the calibration of NASA's Earth Observing System (EOS) sensors. *SPIE Proc.*, **3870**, 180.

[2] Identification of commercial equipment does not imply recommendation or endorsement by the National Institute of Standards and Technology or the National Aeronautics and Space Administration, nor does it imply that the equipment is necessarily the best available for the purpose.

[3] Johnson, B.C., S.S. Bruce, E.A. Early, J.M. Houston, T.R. O'Brian, A. Thompson, S.B. Hooker, and J.L. Mueller, 1996: The Fourth SeaWiFS Intercalibration Round-robin Experiment (SIRREX-4). SeaWiFS Technical Report Series, *NASA Technical Memorandum*, **37**, S.B. Hooker and E.R. Firestone, eds., NASA Goddard Space Flight Center, Greenbelt, MD.


[4] Heath, D.F., Z. Wei, W.K. Fowler, and V.W. Nelson, 1993: Comparison of Spectral Radiance Calibrations of SSBUV-2 Satellite Ozone Monitoring Instruments Using Integrating Sphere and Flat-plate Diffuser Technique, *Metrologia*, **30**, 259.

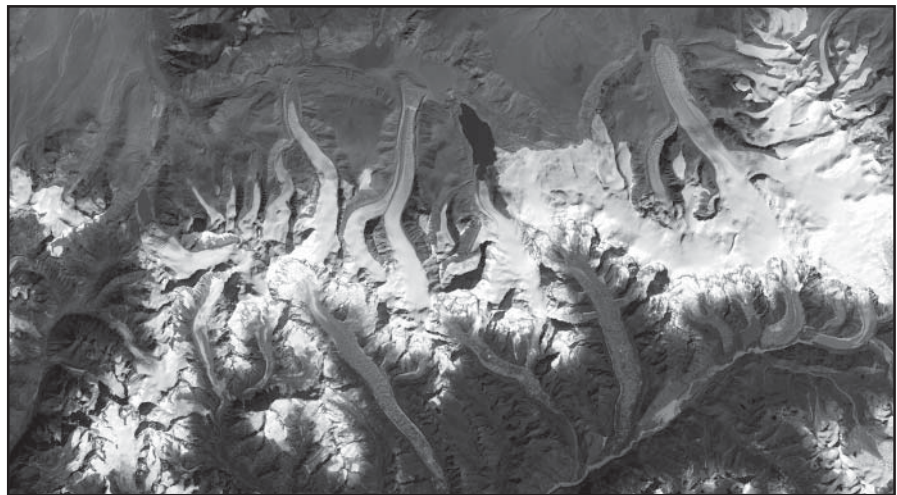
[5] Brown, S.W., and B.C. Johnson, 2002: Development of a portable integrating sphere source for the Earth Observing System's calibration validation program. To appear in *Int. J. Remote Sensing*.

[6] Brown, S.W., G.P. Eppeldauer, and K.R. Lykke, 2002: NIST facility for spectral irradiance and radiance responsivity calibrations with uniform sources. *Metrologia*, **37**, 579.

[7] Marketon, J., P. Abel, J.J. Butler, G.R. Smith, and J.W. Cooper, 2001: A Filter Radiometer Monitoring System for Integrating Sphere Source. *SPIE Proc.*, **4169**, 260.

[8] Butler, J.J., 2000: Radiometric Measurement Comparisons at NASA's Ames Space Flight Center. *The Earth Observer*, **12**, 25.

[9] Pietras, C., M. Miller, R. Frouin, T. Eck, B. Holben, and J. Marketon, 2001: "Calibration of sun photometers and sky radiance sensors." In: G.S. Fargion, R. Barnes, and C. McClain, In Situ Aerosol Optical Thickness Collected by the SIMBIOS Program (1997-2000): Protocols, and Data QC and Analysis, *NASA/TM—2001-209982*, NASA Goddard Space Flight Center, Greenbelt, MD, 11. 



GLACIERS IN FULL RETREAT. According to a joint press release issued by NASA and the U.S. Geological Survey, the great majority of the world's glaciers appear to be declining at rates equal to or greater than long-established trends. This image from the ASTER (Advanced Spaceborne Thermal Emission and Reflection Radiometer) instrument aboard NASA's Terra satellite shows the termini of the glaciers in the Bhutan-Himalaya. Glacial lakes have been rapidly forming on the surface of the debris-covered glaciers in this region during the last few decades.

According to Jeffrey Kargel, a USGS scientist, glaciers in the Himalaya are wasting at alarming and accelerating rates, as indicated by comparisons of satellite and historic data, and as shown by the widespread, rapid growth of lakes on the glacier surfaces. According to a 2001 report by the Intergovernmental Panel on Climate Change, scientists estimate that surface temperatures could rise by between 1.4 and 5.8° C by the end of this century. The researchers have found a strong correlation between increasing temperatures and glacier retreat. **Image Credit:** Jeffrey Kargel., USGS/NASA.

An Introductory Multidisciplinary Set of MODIS Data for the Earth Sciences Community

– Vincent V. Salomonson, vsalomon@pop900.gsfc.nasa.gov, MODIS Team Leader, Goddard Space Flight Center.

Introduction

A special multidisciplinary set of MODIS data products is now available. It is located at: ftp://modis.gsfc.nasa.gov/pub/Data_Sets/ under the descriptor "CDROM".

This data set was prepared to accelerate general knowledge of the availability of consistent, scientifically useful MODIS data products for global modeling and other highly multidisciplinary analyses. This set of coarse-resolution data products will also serve to further inform the general NASA Earth Science community as to the present quality of the MODIS data products. The choice and amount of products provided here are based on several factors: (1) the desire to provide one conveniently sized set of data products that would fit on a CD; (2) to indicate the maturity of the products for scientific use; and (3) to provide enough of the MODIS products to emphasize the breadth and multidisciplinary nature of MODIS data. The data product sets predominantly cover a year extending from November 2000 through October 2001.

It is the opinion of the MODIS Science Team that the majority of the 44 MODIS data products that have been

reprocessed in the period from November 2000 up to the present are scientifically useful. One notable exception is the set of ocean color products for which only a December 2000 data set of selected products is provided. However, another data reprocessing effort (to be completed by the Fall of 2002) should allow all the ocean color products from November 2000 to the

present to achieve scientific utility. The MODIS products are being produced on a continuing basis, and the total suite of products can be accessed via the EOS Data Gateway (EDG): eos.nasa.gov/imswelcome/.

The continuing process of validating the products and their scientific and applications utility is one that should involve the wider user community. Attaining the goal of complete validation is a process wherein one approaches that status somewhat asymptotically depending on the extent and number of validation efforts. Thus, some of the products are further along the path of being validated than others (i.e., aerosols and the 11-micrometer SST products). The MODIS Science Team hopes that the provision of these data products will augment or help the validation process. Certainly, comments on the

TABLE 1: MODIS Atmosphere products (1 degree lat/long grid):

Aerosols (MOD 04)

Total Optical Depth [Over land and ocean]

Ratio of Fine Particle Optical Depth to Total Optical Depth [Over oceans only]

Total water vapor (MOD 05)

Determined by Near-Infrared (NIR) Method

Determined by Thermal Infrared (TIR) Method

Cloud Properties (MOD 06)

Cirrus Fraction [determined by NIR method]

Cirrus Fraction [determined by TIR method]

Cloud Top Pressure

Cloud Top Height

Cloud Particle Phase

Cloud Cover Fraction

Cloud Optical Thickness

Cloud Particle Effective Radius

TABLE 2: MODIS Land Products (0.25 degree lat/long grid):

Surface Reflectance (MOD 09)
 Surface Temperature (MOD 11)
 Normalized Difference Vegetation Index (MOD 13)
 Leaf Area Index/Fraction of Photosynthetically Absorbed Radiation (MOD 15)
 Land Albedo (MOD 43)
 Fire Occurrence (MOD 14)
 Snowcover (MOD 10) [8-day composited intervals]
 Tree Cover (part of MOD44B)

products are welcome and can be sent to the MODIS Science Team Leader – see contact information in title bar.

List of Data Products Provided

The data products that are available are listed in Tables 1-3 on page 9 and 10 – broken down into Atmosphere, Land,

and Ocean Products respectively.

These data are available on CD and are provided principally for the period November 2000 through October 2001. Data are shown as monthly or, in the case of some land products, 32-day composites plotted on linear latitude/longitude, equal distance grids. These same products can be found on an ftp

site: ftp://modis.gsfc.nasa.gov/pub/Data_Sets/.

Suggested software tools

Some basic tools to handle the data are provided to assist with accessing this data. One such tool is operating under windows: Webwinds (see webwinds.jpl.nasa.gov/), and provides basic visualization and analysis of HDF data sets but has not been specifically adapted to the MODIS Multi-disciplinary Data Set.

We provide another tool called HDFLook_MODIS (see www-loa.univ-lille1.fr/~louis/) that is operating under Unix and derivatives (Linux) and has been specifically designed to handle MODIS products (standard and multidisciplinary data set). It will handle visualization and analysis as well as re-projection. All the jpeg images of the land products were generated automatically using HDFLook from the command line using a simple command file. Inputs on suggested improvements to the HDFLook MODIS tool are warmly welcomed.

Additional tools to read and visualize various MODIS products can be found at:

- MODIS Oceans and Atmospheres
Site: daac.gsfc.nasa.gov/MODIS/software.shtml;
- MODIS Land Site: edc.usgs.gov/programs/sddm/modisdist/index.shtml;
- MODIS Snow /Ice Site: nsidc.org/PROJECTS/HDFEOS/MS2GT/.

Future Access to MODIS Data Products

As indicated above, the intent of the provision of a limited set of MODIS

TABLE 3: MODIS Ocean Products (1 degree lat/long grid):

Sea Surface Temperature (MOD 28)

Ocean Color Sampler for December 2000

Water-leaving Radiances (MOD 18)
 Chlorophyll-a Concentration (MOD 19) [empirical]
 Chlorophyll-a Concentration (MOD 21) [semianalytic]
 Chlorophyll-a Concentration (MOD 21) [SeaWiFS analog]
 Fluorescence Line Height (MOD 20)
 Fluorescence Efficiency (MOD 20)
 Calcite Concentration (MOD 25)
 Gelbstoff Absorption Coefficient (MOD 24)
 Phytoplankton Absorption Coefficient (MOD 36)
 Instantaneous PAR (MOD 22)
 Instantaneous Absorbed Radiation by Phytoplankton (MOD 22)


Ocean Primary Productivity (MOD 27)
 Primary Production Index [Behrenfeld-Falkowski model]
 Primary Production Index [Howard-Yoder-Ryan model]
 Mixed-layer Depth

data products is to familiarize the science community with the present state of the products and to provide a useful, introductory data set that could be examined and applied as appropriate for global and interdisciplinary studies. We presume that this data set will result in requests for similar data sets.

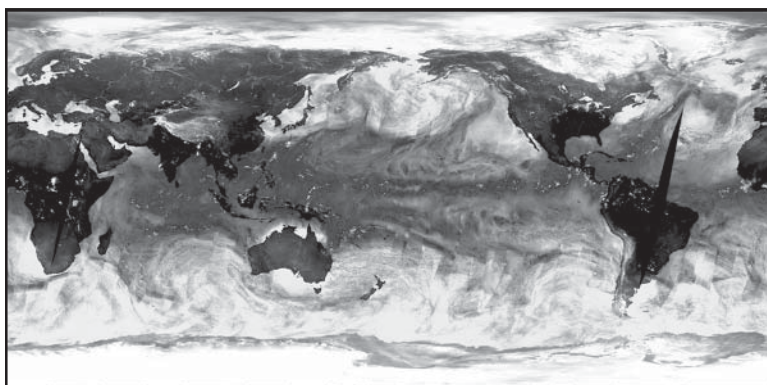
Full resolution data access should be obtained through the EOS Data Gateway (EDG). The EDG strives to evolve and improve access to MODIS products. When users attempt to get MODIS data, it is requested that they

share their experiences with the User Services portions of the Distributed Active Archive Centers (DAACs) that provide MODIS data products. There are three DAAC's involved: (1) the National Snow and Ice Data Center (NSIDC) that provides MODIS snow and ice products; (2) the EROS Data Center (EDC) that provides MODIS land products; and (3) the Goddard Space Flight Center (GSFC) that provides MODIS radiance and geolocation as well as oceans and atmospheres products. By providing comments and suggestions to the User Services components of the DAACs

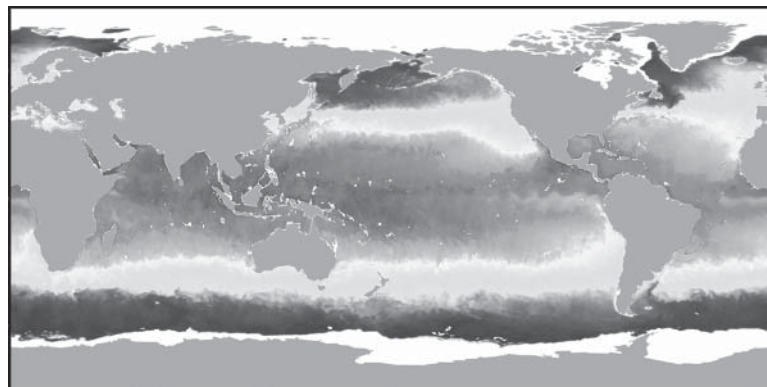
listed above, the EOSDIS Project can take steps to apply resources and energy toward those aspects of MODIS data access that will be the most beneficial to the user community. Again, we urge that users share all comments and suggestions so that we can identify those aspects of the EDG that need to be improved.

In addition to the EDG, users may also access the full-size MODIS-radiance, atmospheres-and-oceans data product files from the GSFC DAAC local user interface at: acdisx.gsfc.nasa.gov/data/dataset/MODIS/ 

First Glimpses from Aqua



(a)



(b)

HIGH  LOW

The Aqua satellite was successfully launched on May 4, 2002. After more than six weeks on orbit, the spacecraft and its six instruments are now sending back its first engineering images. All six instruments have or will soon send back data. The two maps on the left are two engineering images from Japan's Advanced Microwave Scanning Radiometer (AMSR-E).

The map on the top (a) is of the Earth's Brightness Temperature, as measured by AMSR. Ice and snow appear white in this grayscale image, water shows up as lighter shades of gray and land areas tend toward black. The lower image (b) is of sea surface temperature as measured by AMSR. Because AMSR measures microwave radiation, such maps will be made routinely, even in the presence of substantial cloud cover - an improvement over previous SST measurements. Both of the images are provided courtesy of the Japan's National Space Development Agency (NASDA).

Says **Claire Parkinson**, Aqua project scientist at NASA Goddard, "After years of preparation on Aqua, I and hundreds of other scientists are thrilled to have the spacecraft launched and its Earth-observing instruments sending down high-quality data. If all goes as planned, these data will lead to improved weather forecasts and a better understanding of Earth's climate system - especially the role of water in it."

For details and color images, visit aqua.nasa.gov.

Using Landsat Data to Estimate Planted Area and Production Levels of Sugarcane in Argentina

– Federico J. Soria, Carmina del V. Fandos, and Jorge Scandaliaris, *srysig@eeaoc.org.ar*, Estación Experimental Agroindustrial “Obispo Colombes”, Tucumán, Argentina.

Abstract

Using digital information from the Landsat 5 Thematic Mapper (TM) and the Landsat 7 Enhanced Thematic Mapper Plus (ETM+) satellite imagery, the total sugarcane-planted area in the Tucumán Province of Argentina was estimated for the 2001 harvest. Three production levels were differentiated using three different spectral bands of the mapping sensors, and the total harvest was subdivided for each subregion within the province, henceforward referred to as departments.

The crop digital identification was made by analyzing TM and ETM+ images acquired in the month of March 2001, using the Multispectral Supervised Classification method and a software package called *ERDAS Imagine, Version 8.4*. The adopted methodology was shown to be appropriate for the classification of the analyzed area, illustrating the importance of selecting appropriate training fields for later application to areas of interest.

Introduction

Sugarcane is cultivated in the provinces of Tucumán, Jujuy, Salta, Santa Fe, and Misiones in Argentina.

Tucumán is the main producer with more than 60% of all of the country's production. For the sugar industry in Argentina, it is very important to have accurate estimates of sugarcane production prior to harvest to allow for planning for the distribution of the sugar produced, to allow for delivery of the necessary quantity demanded by the national market, and to allow for preparation for shipping the excess quantities of sugar abroad.

Through analysis of Landsat imagery (see the composite image shown in **Figure 1** on the next page) the area for growing sugarcane has been estimated. The production has been differentiated into three levels and results have been calculated for each department in Tucumán province. These activities are part of a larger project developed by Estación Experimental Agroindustrial “Obispo Colombes” (EEAOC) and financed by the Consejo Federal de Inversiones (CFI). The images used were provided by the Comisión Nacional de Actividades Espaciales (CONAE), through a signed agreement with the Production Ministry of Tucumán Province.

Materials and Methods

The following section describes the materials and methods used in the

experiment. Four different steps are involved in the process as discussed in the paragraphs below.

Selection and georeferencing of control fields or training regions

From the cane area, 334 training fields (around 13,100 hectares) have been selected and georeferenced by GPS equipment. The following criteria are applied when choosing a training field:

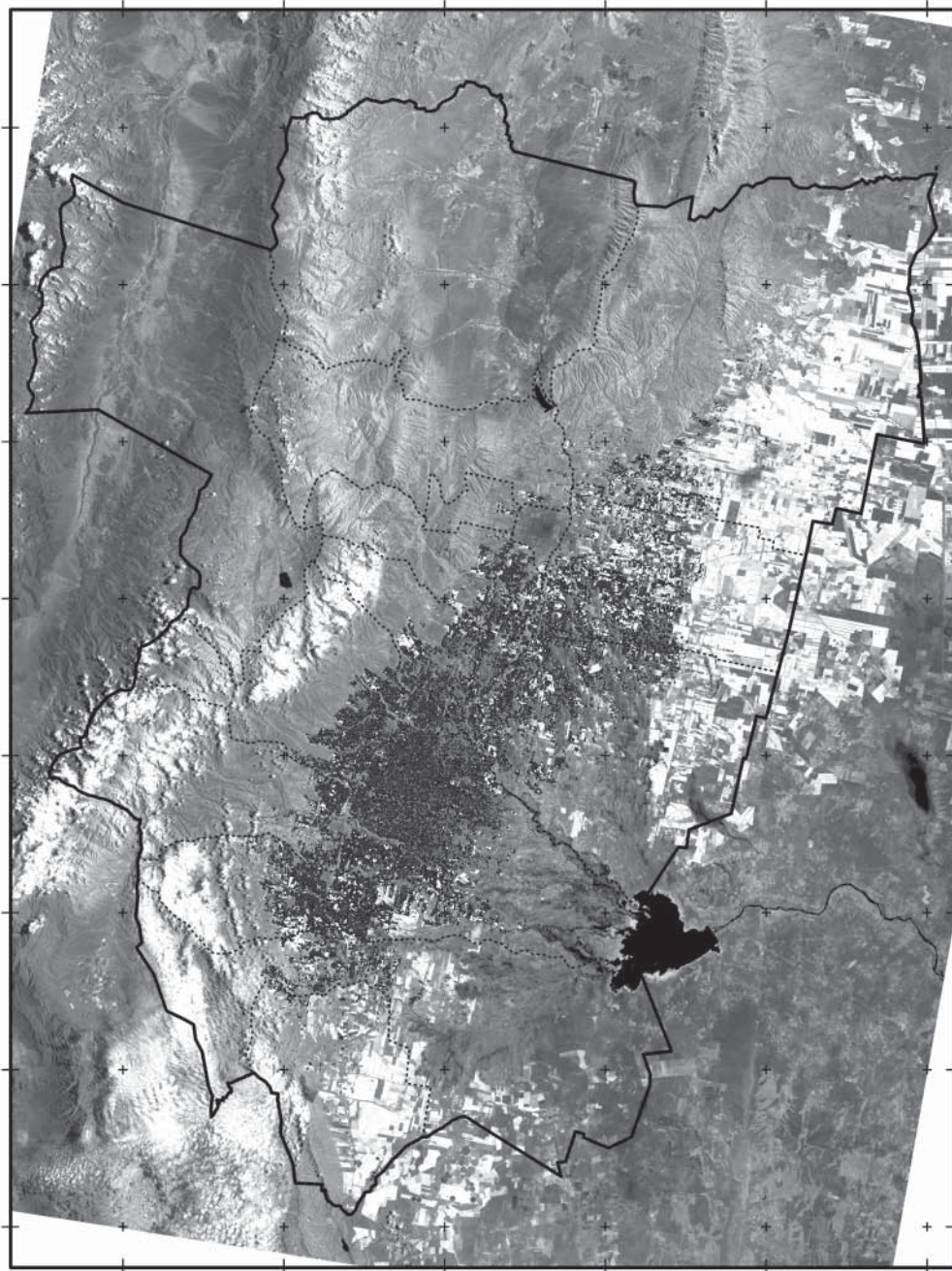
- The provincial subdivision in agricultural regions should individualize the possible behavioral differences of crops in different areas.
- The number of training fields should provide a representative sampling of each agricultural region.
- The size of the cultivated areas should allow their easy identification in the images.

Together with these considerations, additional information about the control fields was entered in a data base and separated in levels of: Area; Company; Department; Location; Section, including a tabulation of the number of furrows; Variety; Age; Estimated Cultural Yield; Irrigation; Fertilization; Latitude; and Longitude.

Selection of images based on the agricultural calendar of the crop

The selected images were taken after the sugarcane had completed its growth period. This is an ideal time for such measurements as the cane plant is still a thick green mass, not yet impacted by chemical treatments or killing frost, allowing for fairly straightforward area estimations. The images used for this experiment are from Landsat 5 and 7. The images were

FIGURE 1: Landsat Image of Sugarcane-Planted Area in Tucumán Province, Argentina - 2001



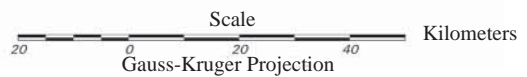
Ministerio de la Producción - C.F.I. - CONAE

Estación Experimental Agroindustrial "Obispo Colombres"

Multispectral Classification: Uses images from Landsat 5 TM, Orbital 231, Row 78-79 and Landsat 7 ETM+, Orbital 230, Row 78-79. Images acquired March 28-29, 2001.

Image Credit: Federico Soria and Carmina Fandos, Sección Sensores Remotos y S.I.G., May 2001.

Production Levels , See Table 1



obtained on March 28th and 29th, 2001. The Landsat 5 image is of path 231/ rows 78-79 and the Landsat 7 image is of path 230/ rows 78-79, from the worldwide reference system.

Field conditions in the training fields, at time of overpass

The conditions in the field (moisture of soil for example) can have an impact on the spectral properties of the sugarcane plants and alter the spectral response. Therefore, it was necessary to carefully observe the conditions in the field at the time of each observation.

Digital interpretation and classification of selected images

ERDAS Imagine, Version 8.4 was used to obtain a Multispectral Supervised Classification. The Landsat instruments

collect information in seven spectral bands. Bands 3, 4, and 5 were used for this experiment because, by combining the information from these three bands, one is able to discriminate between different species of vegetation and varying amounts of biomass. The nominal ground sample size of bands 3, 4, and 5 on both Landsat 5 and Landsat 7 is 30 m. The half-amplitude widths of the bands on both satellites are: Band 3 (0.63-0.69 μm), Band 4 (0.76-0.90 μm), Band 5 (1.55-1.75 μm).

The classification begins by selecting spectral signatures. This involves the following activities:

- Obtain spectral signatures over “control” fields of uniform vegetation to obtain crop spectral signatures for each different

vegetation type in the study and look at each vegetation type over a range of yield rates.

- Obtain spectral signatures in the selected region with mixed vegetation.
- Compare observed signatures with “control” signatures and select representative signatures for the different yield ranges.
- Compare spectral selected signatures for the same yield range. Account for different plant species, according to the available field information.

Figure 2 demonstrates the difference in digital levels obtained by the three bands used in this experiment. The graph on the left (a) is for Landsat 5 and the graph on the right (b) is for Landsat 7. It becomes apparent that for

FIGURE 2

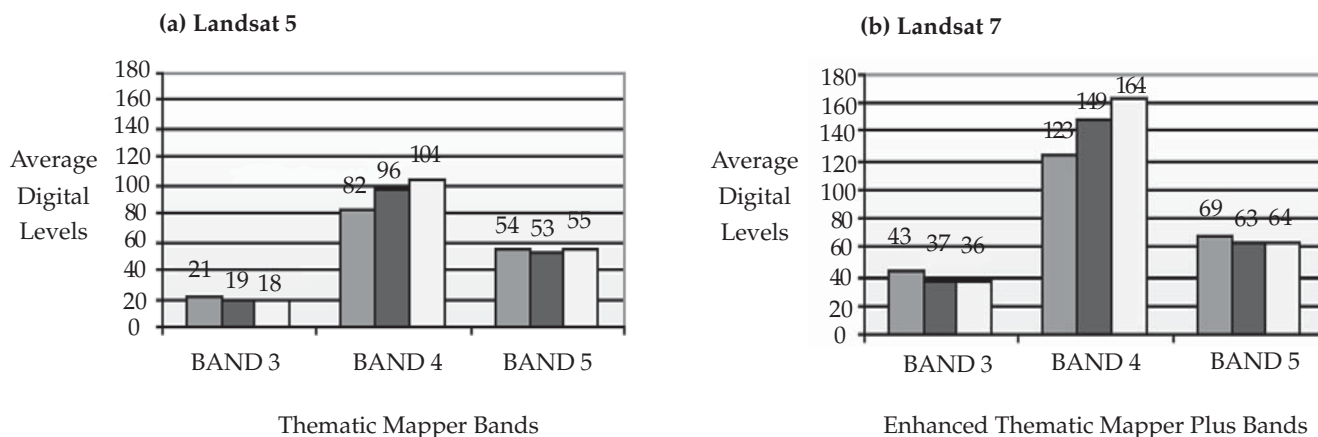


FIGURE 2 demonstrates the difference in digital levels obtained by the three bands used in this experiment. The graph on the left (a) is for Landsat 5 and the graph on the right (b) is for Landsat 7. The bar graphs illustrate that for the sensors on both instruments (TM and ETM+, respectively) Band 4 is most useful for distinguishing between varying production levels – low, medium, and high. The other bands are far less distinctive.

Production Level
 ■ LOW ■ MED □ HIGH

TABLE 1: Definitions of Yield Categories used in this Experiment

Yield Category	Classification (t/ha)	Total Area in Hectares (ha)
Low Yield	56	128,780
Medium Yield	57-75	45,940
High Yield	76	8,670

both TM on Landsat 5 and ETM+ on Landsat 7, Band 4 is most capable of distinguishing between scenes with varying yield. Band 5 is less distinctive and in Band 3, the changes are almost negligible.

This classification scheme was applied to each path and a definite spectral signature was determined for each image.

Results

The raw area devoted to sugarcane growth in the year 2001 was estimated at **215,750 hectares**. About 15% of the total area covered by sugarcane is not cultivated, so there are approximately 183,390 hectares of net area being used. Sugarcane yield is classified into three production levels (low, medium, and high) according to the distinctions in **Table 1**.

In terms of percentages, 70% of the planted area is classified as low yield, 25% is classified as medium yield, and 5% is classified as high yield. **Figure 1** shows a thematic map indicating that the high-yield regions are concentrated in the northeast and south of the sugarcane area. The medium-yield regions are grouped around the regions of higher yield, mainly to the east of

Salí river and to the south of Gastona river, while most of the area with low yield is in the central part of the region.

Breaking the sugarcane production down to examine how much each department produces (see **Table 2**) reveals that 15 of the 16 departments in the Tucumán Province had sugarcane plantations. **Table 2** shows the estimated total sugarcane area in each department and breaks it down to show how much comes from high-, medium-, and low-yield regions respectively.

The classification scheme is validated by examining relationships between crops in "control" regions, not used to obtain the spectral signatures, with the results given by the classification for

TABLE 2: Total Sugarcane Harvest in Tucumán Province By Department

Department	Low Yield (ha)*	Medium Yield (ha)*	High Yield (ha)*	Total (ha)*
Cruz Alta	16,460	15,570	5,710	37,740
Simoca	25,270	5,360	250	30,880
Leales	21,990	6,720	690	29,400
Monteros	18,550	1,620	30	20,200
Chicligasta	11,790	1,700	40	13,530
Rio Chico	9,940	3,190	220	13,350
Burruyacu	4,630	4,230	960	9,820
Lules	6,310	1,870	130	8,310
Famailla	6,720	1,100	50	7,870
J.B. Alberdi	4,670	2,420	350	7,440
La Cocha	940	1,210	90	2,240
Graneros	990	580	100	1,670
Tafi Viejo	330	190	30	550
Yerba Buena	150	130	10	290
Capital	40	50	10	100
TOTAL	128,780	45,940	8,670	183,390

* : Net Area

those same fields and also by independent “ground truth” observations of the conditions in the region.

The results indicate an error of $\pm 5\%$. It was verified that areas having estimated yields lower than 400 kg/furrow were not classified. These areas are mainly concentrated in the “low plain” zone. The errors mainly occurred in regions with second-growth trees and in regions with humid soil found on the plains.

Conclusions

The following are the findings of this study:

- The failure to classify areas with less than 400 kg/furrow caused errors beyond those acceptable for the project’s goals.
- This study builds on the experience obtained in previous campaigns. The Multispectral Supervised Classification was the correct methodology to use for this study. Previous knowledge of the characteristics of this country’s

regions was very important in selecting the training fields.

- Though the spectral signature extraction was done during a phase of sugarcane growth characterized by uniform vegetative cover, the models developed for this study should still only be considered valid for the images used in this work.

References

Bähr, H. P. 1991: Procesamiento Digital de Imágenes, Aplicaciones en Fotogrametría y Teledetección. Alemania.

Chuvieco, E. 1990: Fundamentos de Teledetección Espacial. Madrid. España.

Gastellu Etchegorry, J. P. 1990: Satellite Remote Sensing for Agricultural Projects. World Bank Technical Paper Number 128. Washington. Estados Unidos.

Hellmann, D. B., M. G. Wallace, and G.


G. Platford 1995: Interpreting farm sugarcane yields using a geographic information system (GIS). *Proceedings*

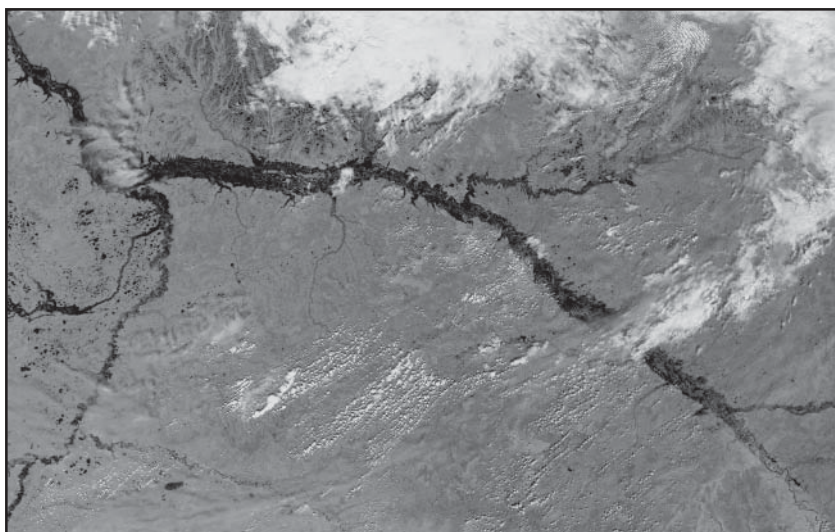
of The South African Sugar Technologists’ Association. Sudáfrica.

Lee-Lovick, G. and L. Kirchner 1991: Limitations of Landsat TM data in monitoring growth and predicting yields in sugar cane. *Proceedings of Australian Society of Sugarcane Technologists.* Australia.

Scandaliaris, J. et al. 1997: Empleo de imágenes satelitales para el relevamiento del área cañera de la provincia de Tucumán. Avance Agroindustrial E.E.A.O.C. Tucumán. Argentina.

Soria F. J. and C. Fandos 1999: Relevamiento satelital de la Provincia de Tucumán, determinación del área cultivada con citrus y granos, y producción de caña de azúcar. E.E.A.O.C. – C.F.I. Tucumán. Argentina.

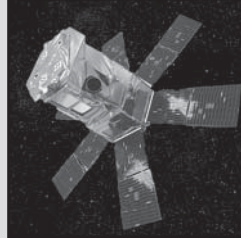
Zuccardi, R. B. and G. Fadda, 1985: Bosquejo Agroecológico de la Provincia de Tucumán. Miscelánea 86. Facultad de Agronomía y Zootecnia de la U.N.T. Tucumán. Argentina. 



MODIS VIEWS FLOODING IN WESTERN SIBERIA. A mixture of heavy rainfall, snowmelt, and ice jams in late May and early June of this year caused the Ob River and surrounding tributaries in Western Siberia to overflow their banks. The flooding can be seen in this image taken on June 16, 2002, by the MODIS (Moderate Resolution Imaging Spectroradiometer) instrument aboard the Terra satellite. Last year, the river flooded farther north. Normally, the river resembles a thin black line. **Image Credit:** Jacques Desclotres, NASA-GSFC.

An Overview of the Solar Radiation and Climate Experiment (SORCE)

- Gary Rottman, *gary.rottman@lasp.colorado.edu*,
University of Colorado, Laboratory for Atmospheric and Space Physics
- Vanessa George,
vanessa.george@lasp.colorado.edu, *University of Colorado, Laboratory for Atmospheric and Space Physics*



Mission Overview

The Solar Radiation and Climate Experiment (SORCE) is a free-flying satellite carrying four instruments that will measure the solar radiation incident at the top of the Earth's atmosphere. SORCE is one element of the Earth Observing System (EOS) and is scheduled for launch in November 2002. The Laboratory for Atmospheric and Space Physics (LASP) at the University of Colorado has full programmatic responsibility for the SORCE mission, which is under the direction of Principal Investigator Gary Rottman. This mission builds on a rich heritage of total solar irradiance (TSI) measurements that began with the ERB instrument in 1978 and have continued to the present with the ERBS, ACRIM, and VIRGO measurements. SORCE will also provide spectral irradiance measurements over the entire range of solar wavelengths from 1 to 2000 nm. SORCE will carry four instruments into space, each designed to study different wavelengths of solar radiation. These include the Total Irradiance Monitor (TIM), the Spectral Irradiance Monitor (SIM), two Solar Stellar Irradiance Comparison Experiments (SOLSTICE), and the XUV Photometer System (XPS). Solar radiation, the Earth's average

albedo, and longwave infrared emission determine the Earth's global average equilibrium temperature. Measurements obtained during the past 22 years show that TSI varies ~0.1% over the solar cycle with somewhat larger short-term variations. The variations occur over time scales from a day up to and exceeding the 11-year solar cycle. (Figure 1 depicts conditions on the sun during a time of maximum solar activity.) Climate models including a realistic sensitivity to solar forcing indicate corresponding global surface temperature changes on the order of 0.2°C for recorded solar variations. However, global energy balance considerations may not provide the entire story, and how TSI variations are distributed in wavelength is critically important in understanding the Earth's response to solar variations.

Because of selective absorption and scattering processes in the Earth's atmosphere, different regions of the solar spectrum affect our environment in distinct ways. Approximately 20-25% of the TSI is absorbed by atmospheric water vapor, clouds, and ozone, impacting convection, cloud

formation, and latent heating processes. All of these processes are strongly wavelength dependent.

Wavelengths below 300 nm are completely absorbed by the Earth's atmosphere and contribute the dominant energy source in the stratosphere and thermosphere, establishing the upper atmosphere's temperature structure, composition, and dynamics. Variations in the Sun's radiation at these short wavelengths can be factors of two or even greater and lead to significant changes in atmospheric chemistry. Solar ultraviolet radiation influences stratospheric chemistry and dynamics, which in turn control the amount of ultraviolet radiation (UVB) reaching the surface.

The bulk of solar radiation falls in the visible and near-infrared region of the electromagnetic spectrum and pen-

FIGURE 1

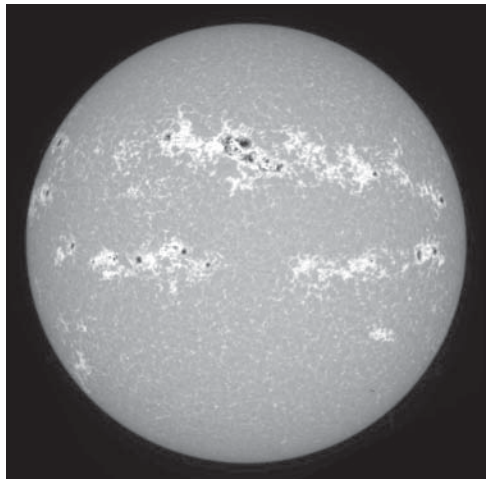


FIGURE 1 is a picture of the solar disk that depicts conditions that are typically observed on the sun during a period of maximum solar activity. The dark regions are the sunspots, and the bright regions are the faculae associated with current or old sunspots. In contrast, there would be few, if any, of these active regions during a period of minimum solar activity. The SORCE mission will study the impact that variations in solar activity have on the Earth's climate and continues a long standing record of similar measurements obtained by previous missions.

etrates into the lower atmosphere. The non-reflected portion of this radiation is absorbed in the troposphere or by the Earth's surface, becoming a dominant term in the global energy balance and an essential determinant of atmospheric stability and convection. To understand the effects of solar variability on Earth's climate, it is important to accurately monitor both the TSI and its spectral dependence.

SORCE Science Objectives

SORCE will make precise and accurate measurements of the TSI. These measurements will be connected with previous TSI measurements to continue a long-term record of solar influences on the Earth. SORCE will measure TSI with an absolute accuracy of 0.01% and with a long-term relative accuracy of 0.001% per year.

SORCE will also make precise measurements of the visible and near-infrared solar spectral irradiance suitable for future climate studies. In addition, SORCE will obtain daily measurements of the solar spectral irradiance from 300 to 2000 nm with a spectral resolution ($\lambda/\Delta\lambda$) of > 30 nm, an absolute accuracy of 0.03%, and a precision and relative accuracy of better than 0.01% per year.

In addition, SORCE will make daily measurements of the solar ultraviolet irradiance from 115 to 320 nm with a spectral resolution of 0.1 nm. It will achieve this measurement with an absolute accuracy of better than 5% and with a long-term relative accuracy of 0.5% per year. The satellite will use stellar observations and compare the solar spectral irradiance to the ensemble average flux from a number of bright, early-type stars.

A complete listing of the required capabilities of each instrument and the actual capabilities of each instrument is given in **Table 1** on page 17. The SORCE observations will improve our understanding of how and why solar variability occurs and how it affects our atmosphere and climate. Scientists will use this knowledge to estimate past and future solar behavior and climate response.

The SORCE Instruments

SORCE carries a suite of four instruments which are discussed in detail below. A photograph of each instrument can be found in **Figure 2** on page 19. **Figure 3** at the top of page 20 shows the solar spectrum and indicates the spectral range for each instrument on SORCE.

Total Irradiance Monitor (TIM)

The TIM, shown in **Figure 2(a)**, will provide a measurement of total solar irradiance (TSI) directly traceable to SI units with an absolute accuracy of 0.01% and relative stability of 0.001% per year. This instrument will monitor the Sun every spacecraft orbit, reporting four TSI measurements per day. These data provide the radiative input at the top of the Earth's atmosphere needed for climate models. The TIM will continue a 24-year record of spacecraft TSI measurements with improved absolute accuracy. This new instrument takes full advantage of the best heritage of previous radiometers, but is enhanced with modern state-of-the-art technologies including phase-sensitive detection, metallic absorptive materials, digital electronics, and diamond electrical/thermal nodes.

The TSI, sometimes erroneously called the solar "constant," is approximately 1366 W/m^2 at 1 AU, but has average

variations of 0.1% through an 11-year solar cycle. Changes in TSI over the last 150 years may be responsible for 1/3 of the Earth's climate warming.

The TIM measures solar irradiance with four Electrical Substitution Radiometers (ESR's). The ESR's are absorptive black cavities that are maintained at a fixed temperature by applying a known amount of electrical power. A shutter in front of each ESR controls incoming light. When sunlight is absorbed by an ESR, less electrical power is required to maintain its temperature; this decrease indicates the incident sunlight power. A precision aperture behind the shutter defines the area over which sunlight is collected, and the power per unit area gives the solar irradiance.

The TIM achieves extremely low noise using phase-sensitive detection at the shutter fundamental. This detection method reduces sensitivity to thermal drifts, $1/f$ noise, and thermal emission from the instrument. The process involves shuttering the sunlight, processing through a linear system, and Fourier-transforming the signal to get the component at, and in-phase with, the shutter fundamental. This method improves the signal/noise ratio compared to traditional time-domain analysis, as the noise at frequencies and phases other than the fundamental does not affect the measurement. Using this technique, TIM has demonstrated noise levels less than 0.0002%.

To monitor the stability of the cavity absorptance, the TIM will duty-cycle the four ESR's in flight to characterize degradation. Comparisons of nearly simultaneous measurements with each ESR will indicate cavity absorptance changes attributable to solar exposure.

FIGURE 2

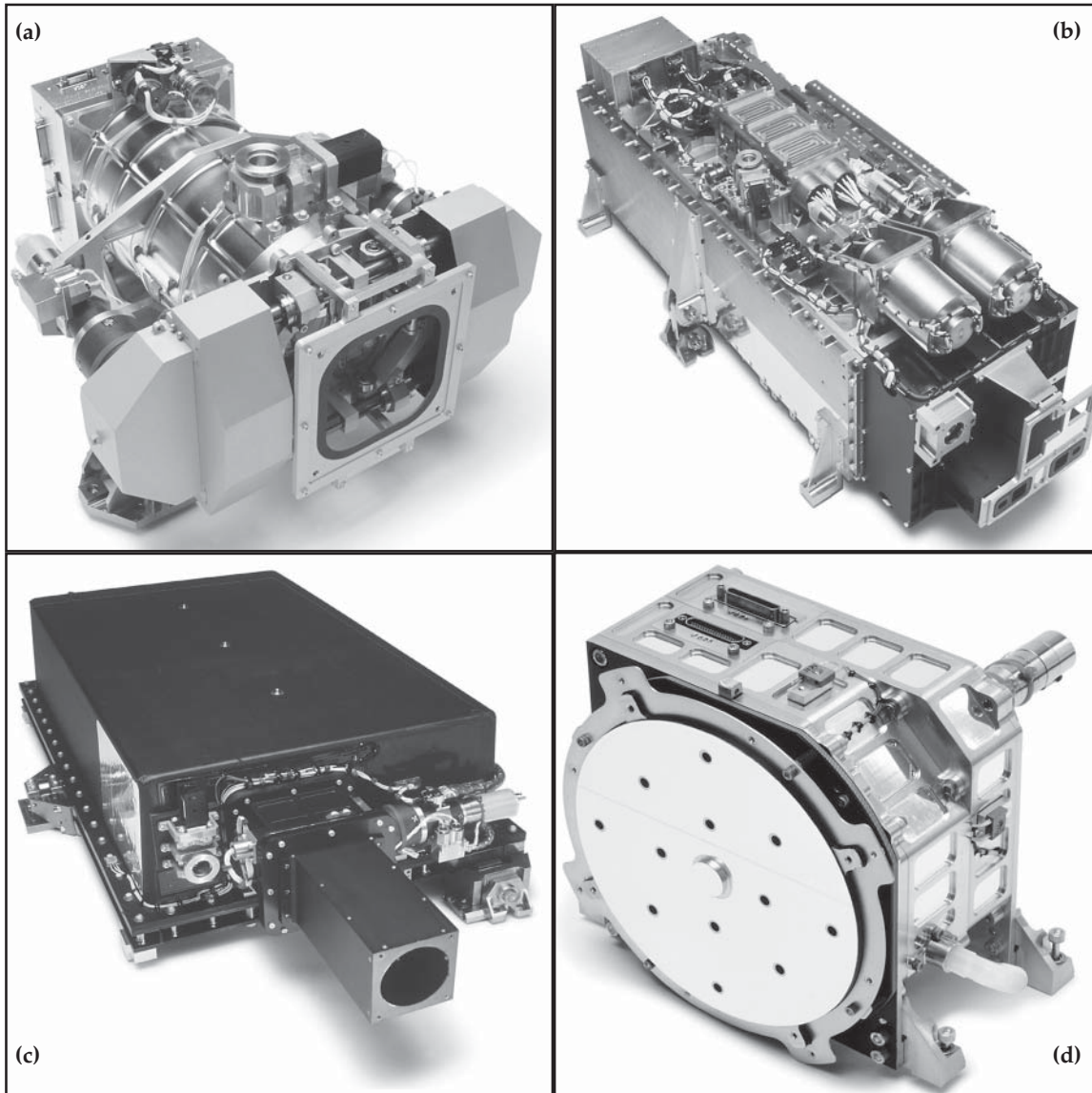


FIGURE 2 shows the four instruments that will fly onboard SORCE. Each instrument will take measurements in a different region of the solar spectrum as shown on the graph on the next page. In the upper left (a) is the Total Irradiance Monitor (TIM), which will measure total solar irradiance and covers the entire solar spectrum. In the upper right (b) is the Spectral Irradiance Monitor (SIM), which obtains measurements in the visible and near infrared regions of the spectrum. In the lower left (c) is the Solar Stellar Irradiance Comparison Experiment (SOLSTICE), a grating spectrometer that will measure spectral irradiance in the ultraviolet region from 115-320 nm. Finally, in the lower right (d) is the XUV Photometer System, which will measure solar soft X-ray (XUV) irradiance from 1-34 nm and also will measure the bright hydrogen emission at 121.6 nm (H I Lyman- α). **Photos Taken By:** Geoffrey Wheeler Photography.

FIGURE 3

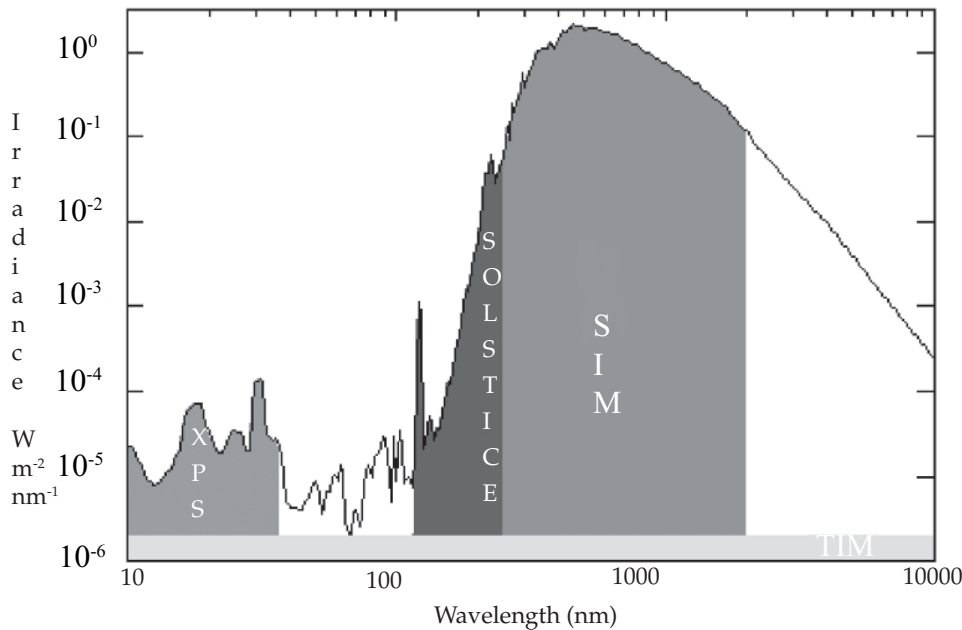


FIGURE 3 shows a log-log plot of the solar irradiance spectrum. The shaded regions indicate the spectral regions for the four instruments that will fly onboard SORCE.

Spectral Irradiance Monitor (SIM)

This newly designed spectrometer, shown in **Figure 2(b)**, will provide the first long-duration measurements in the visible and near infrared spectral regions. The SIM will measure spectral irradiance primarily from 300 to 2000 nm with an additional channel to cover the 200-300 nm region to overlap with SOLSTICE. Solar variability models predict very small fractional changes, on the order of 0.1-0.01%, in the solar output over this spectral range; nonetheless, understanding its wavelength-dependent variability is of primary importance for long-term climate-change studies here on Earth.

The SIM instrument design was conceived as a replacement for the UARS SOLSTICE N-channel spectrometer. SIM employs a single optical element, prism spectrometer and an electrical substitution radiometer to allow much broader wavelength

coverage and traceability to SI standards of radiometric power.

The prism has a concave front surface and a convex, aluminized back surface that focuses and disperses the light beam onto the instrument focal plane

that contains the ESR and four additional photodiode detectors. The prism spectrometer has a resolution varying from 0.2 to 33 nm. SIM contains two completely independent and identical (mirror-image) spectrometers to provide the redundancy, self-calibration capability, and duty cycling needed to meet the scientific objectives over the duration of the SORCE mission. Theory and modeling of solar radiation, with the additional constraint of past TSI observations, predict a very small fractional change for the visible/NIR region of the solar spectrum. The design goal for visible light measurements is therefore 0.03% absolute and a relative accuracy of 0.01% per year.

The SIM ESR operates on the same principle and uses the same detector methodology as the active cavity radiometer for TIM. However, the light signals at the focal plane of the spectrometer are ~1000 times smaller, so a

TABLE 1: SORCE Instrument Requirements and Capabilities

Attribute	TIM	SIM	SOLSTICE	XPS
Spectral Range	Full Spectrum	200-2000 nm	115-320 nm	1-31 nm
Spectral Resolution	N/A	0.2-33 nm	0.1 nm	5-10 nm
Cadence (Reported)	4 per day	4 per day	4 per day	4 per day
Absolute Accuracy (1 σ), Measured	100 ppm	300 ppm	3-5%	12-20%
Absolute Accuracy, Required	150 ppm	1500 ppm	0.5-10%	30%
Relative Accuracy (1 σ), Measured	10 ppm/yr	100 ppm/yr	< 0.5%	< 3%/yr
Relative Accuracy, Required	10 ppm/yr	100 ppm/yr	< 0.5%	< 3%/yr
Precision (1 σ)	< 1 ppm	< 150 ppm	< 0.5%	< 2%

different thermal/mechanical design is used for this detector. Instead of using a cone to absorb radiation, a bolometer made of synthetic diamond is blackened with nickel phosphorous black (NiP) to absorb the spectral radiation. Change in temperature induced by this radiation is detected by thermistors located at each end of the diamond strip and an integrated thin film heater supplies the “substitution” power. Two of these bolometers are located inside a small spherical cavity; the active bolometer sees light from the spectrometer while the reference does not. The thermistors on the two bolometers are part of a precision AC bridge circuit that maintains an equal temperature on the two bolometers; bridge balance is achieved by varying the duty cycle of the power applied to the active bolometer. As in the TIM instrument, a shutter modulates the input light beam, and the ESR time series data are analyzed in the frequency domain at the shutter fundamental frequency.

The spectrometer requires precision motion of the prism to achieve a wavelength error $\delta\lambda/\lambda < 150$. This requirement is met by a closed-loop wavelength-drive system employing a voice coil-actuated turntable to rotate the prism and a Charged Coupled

Device (CCD) linear array in the spectrometer’s focal plane to detect the prism rotation angle. The two SIM spectrometers can be coupled with a periscope that images one prism onto the other. When they are coupled to the periscope, light from one spectrometer can then be used as a monochromator to make in-flight measurements of the other spectrometer’s prism transmission.

Solar Stellar Irradiance Comparison Experiment (SOLSTICE)

SOLSTICE, shown in **Figure 2(c)**, is a second generation of the UARS SOLSTICE also built by LASP, and successfully operating for more than 10 years. This grating spectrometer will measure spectral irradiance from 115 to 320 nm with a resolution of 0.1 nm, an absolute accuracy of better than 5%, and a relative accuracy of better than 0.5%. The instrument observes the Sun and bright, early-type stars using the very same optics and detectors used on the UARS SOLSTICE. The stellar targets establish the long-term corrections to the instrument sensitivity. The ensemble average flux from these 20 stars should remain absolutely constant (intrinsic variability of less than one part in ten thousand over thousands of years). This in-flight calibration technique establishes the instrument response as a function of time throughout the SORCE mission, yielding solar data that are fully corrected for instrumental effects to an accuracy of about 1%. Moreover, the SOLSTICE technique provides a method of directly comparing solar irradiance measurements made during the SORCE mission with previous (e.g., UARS SOLSTICE) and future observations. The same set of stable stars selected by UARS, based on repeated observations throughout the 10-year

mission (1991 to present), will be continued for the SORCE mission.

XUV Photometer System (XPS)

The XPS, shown in **Figure 2(d)**, measures the solar soft X-ray (XUV) irradiance from 1 to 31 nm and the bright hydrogen emission at 121.6 nm (H I Lyman- α). The solar XUV radiation is mostly emitted from the hot, highly-variable corona on the sun, and these high-energy photons are a primary energy source for heating and ionizing Earth’s upper atmosphere. Of all the SORCE instruments, the XPS is most sensitive to flare events on the sun as the solar XUV radiation often changes by a factor of 2 to 10 or more during flares.

With the launch of Solar & Heliospheric Observatory (SOHO) in 1995, Student Nitric Oxide Explorer (SNOE) in 1998, and Thermosphere-Ionosphere-Mesosphere-Energetics-Dynamics (TIMED) spacecraft in 2001, there is now a continuous data set of the solar XUV irradiance, and advances in the understanding of the solar XUV irradiance have begun. The SORCE XPS, which evolved from earlier versions flown on SNOE and TIMED, will continue these solar irradiance measurements with improvements to accuracy, spectral range, and temporal coverage.

XPS contains a set of twelve photometers consisting of Si photodiodes with thin-film filters, each having a spectral bandpass of about 7 nm. These filtered Si photodiodes have proven to be very stable over long time periods and with extended exposure and have been adopted by the National Institute of Standards and Technology (NIST) as secondary radiometric detector standards.

FIGURE 4

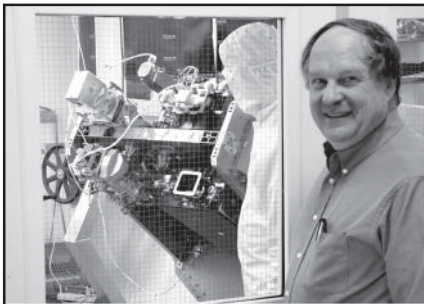


FIGURE 4 shows the SORCE instrument module in the cleanroom at LASP. SORCE Scientist, George Lawrence, is pictured in the foreground.

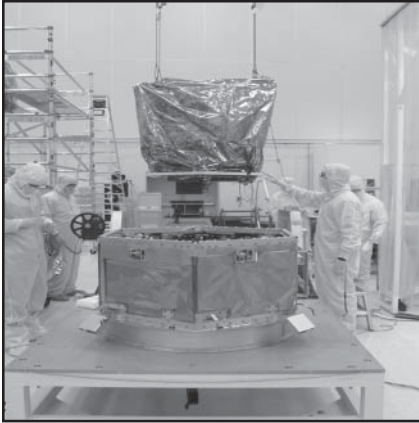
FIGURE 5

FIGURE 5 shows the instrument module being integrated with the SORCE spacecraft at the Orbital facility in Dulles, Virginia.

Mission Status

SORCE sponsored an Open House and Press Conference at LASP in February to celebrate the completion of years of hard work developing and building the four SORCE instruments. The instruments were integrated on the instrument module (IM) in the LASP cleanroom (shown in **Figure 4**) before their final delivery to Orbital Sciences Corporation in Dulles, Virginia. Orbital is under contract by LASP to provide the spacecraft bus and instrument integration (shown in **Figure 5**) in preparation for the November 2002 launch. Packed in sealed vibration- and shock-resistant metal containers free from dust and other contaminants, the instruments were loaded into a truck for the 1600-mile journey from Colorado to Orbital. After arrival at Orbital's Dulles facility, the units were unpacked, powered up, and the integration and testing phase began in early March.

The first week in April, the instrument alignment process began. Only one of the five instruments required a slight adjustment. The SORCE Software Team loaded new flight code in the microprocessor unit in mid-April, and

the code verification test passed with flying colors. On April 16, the SORCE instrument module was successfully mated to the spacecraft bus. By the end of April everything was ready for Spacecraft Test.

The instruments underwent Comprehensive Performance Testing (CPT) during May. On May 7, the Fault Detection and Correction (FDC) Review was conducted and the Pre-Environmental Readiness Review (PERR) occurred at the end of May. Additional environmental tests will continue throughout the summer in preparation for shipment of the satellite to Kennedy Space Flight Center (KSC), Cape Canaveral, Florida. These tests include vibration, EMI/EMC measurement, mass properties, pyroshock separation system, thermal vacuum, and acoustics. Currently, these tests are going very well with no significant unexpected results. Once the launch vehicle and payload are transferred to KSC, the two will be mated and prepared for launch.


The SORCE satellite will be launched from a Pegasus® XL in November 2002. Orbital's Pegasus launch vehicle is an air-launched, internally guided, 3-stage solid rocket capable of launching up to 1,000 lbs. to Low Earth Orbit (LEO). Pegasus is mated to its L-1011 carrier aircraft and dropped at approximately 38,000 feet. The vehicle free falls for approximately 5 seconds, with its delta wing providing lift, before firing its first stage rocket motor. The duration of a typical flight, from drop to insertion into orbit, is approximately 11 minutes.

LASP's Mission Operations Center (MOC) in Boulder, Colorado, will be responsible for command and control of the satellite and mission science

planning. The MOC is prepared to operate and obtain data from the SORCE spacecraft for a period of 5 years (6-year goal), and to process and analyze all engineering data to insure the health and safety of the spacecraft and instruments. NASA's Space/Ground Network, through antenna sites at Wallops Island, Virginia, will provide the communication link to the satellite. Within 48 hours of data capture, all science data with the associated instrument and spacecraft engineering data will be processed to derive Level 3 science data products in standard geophysical units (W/m^2 or $W/m^2/nm$). The Level 3 data are 6-hr averages, with higher time-resolution data available to meet secondary science objectives such as studying the passage of faculae and sunspots across the solar disk. Validated data will be provided to the scientific community within 3 months after data acquisition. The SORCE data will be validated against other simultaneous space observations (when available), against previous spectral irradiance observations, and against the best-known models of solar radiation.

Acknowledgements

The authors would like to acknowledge the following individuals for their contributions to the SORCE mission.

- **SORCE Team Members:** Jerry Harder, Greg Kopp, George Lawrence, Bill McClintock, Tom Woods, Mike Anfinson, Tom Sparn, Rick Kohnert. All are at LASP, University of Colorado.
- **SORCE Project Scientist:** Robert Cahalan – NASA Goddard Space Flight Center.
- **SORCE Project Manager:** William Ochs – NASA Goddard. 

Mixed Croplands May Make Some Areas Cooler, Wetter in Summer

Cynthia M. O'Carroll, cynthia.m.ocarroll.1@gssc.nasa.gov, Goddard Space Flight Center, Greenbelt, Md.

Krishna Ramanujan, kramanuj@pop900.gssc.nasa.gov, Goddard Space Flight Center, Greenbelt, Md.

The variety of the vegetation and crops in the Great Plains and Rocky Mountain states has helped maintain a cooler, wetter climate, according to a NASA-funded study using a computer climate model.

Hydrometeorologists Jim Shuttleworth at the University of Arizona, Tucson, Ariz., and Lixin Lu at Colorado State University, Fort Collins, Colo., found that when they introduced satellite measurements of the real patterns of vegetation in Great Plains and Rocky Mountain states into a computer model, the results generated extra convection in the atmosphere to give a cooler, wetter climate.

The report appears in the June issue of the *Journal of Hydrometeorology*. The study found that mixed vegetation impacts the atmosphere and the weather and climate through the proportion of sunlight that gets reflected from the land and leaves back out to space, the varying heights of trees and other plants exposed to the wind, and the effectiveness of different plant types, when it comes to evaporating water.

For example, irrigated, lush crop lands with plenty of water in the soil warm the air less because they use more of the Sun's energy for evaporation, as

compared to hot, dry bare soil. Along with differing temperatures, the varied heights of plants and trees in a region change the aerodynamics of the atmosphere, creating more circulation and rising air. When the rising air reaches the dewpoint in the cooler, upper atmosphere, it condenses into water droplets and forms clouds. "The mixed vegetation creates areas of different temperatures next to each other, some warmer and some colder, and this leads to mixing in the atmosphere that gives rise to clouds and, ultimately, rain," Shuttleworth said. Over the last two decades, detailed maps of the amount and type of vegetation that covers the ground have become available through remote sensing. Based on that information, scientists can enter data to describe vegetation into computer models that simulate regional climate.

In this study, a climate version of the Regional Atmospheric Modeling System (ClimRAMS) was used to explore whether more of a mix of vegetation can alter climate in the United States.

A U.S. Department of Agriculture soil database was used to define different soil types in the climate model, and vegetation was classified using an international land-cover system.

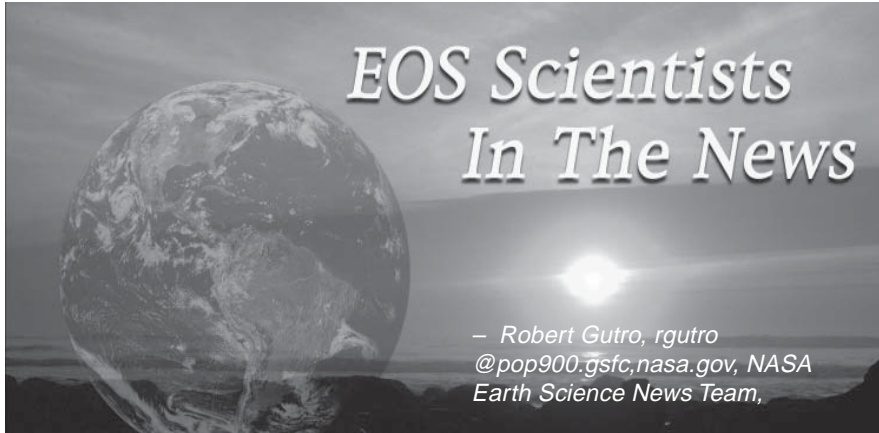
The ClimRAMS normally assumes there is little difference between grasslands in northern Wyoming and southern Kansas, for instance, but the researchers found that when they introduced satellite measurements of "leaf area index" (a way of quantifying how much vegetation is actually present), the more realistic pattern of vegetation generated extra convection in the atmosphere to give a cooler, wetter climate.

Shuttleworth and Lu used satellite plant cover data from Kansas, Nebraska, South Dakota, Wyoming, and Colorado for their computer model runs. Computer model simulations of the growing season that included satellite data of mixed vegetation showed lower maximum and minimum temperatures in the region, compared to a model run that contained less detail of plant cover. Over the entire year, simulated precipitation levels were on average two-thirds of a millimeter per day more for the model using mixed vegetation, which may account for the cooler temperatures found during the growing season.

In general, most current computer models that predict Earth's future climate do not account for the complex mix of vegetation and its atmospheric impacts, and may be producing forecasts that are too dry and too warm during growing seasons. "In the future, it will be important to use remote sensing data to enter the fine details of plant cover into computer models to get more accurate weather and climate forecasts," Shuttleworth said. Further, more research is needed to determine if increasing the variety of croplands would help lessen drought conditions.

This research was funded by the NASA Land Surface Hydrology Program.





Spotlight on the AGU -The Spring Meeting of the American Geophysical Union, held at the end of May 2002, featured 5 NASA-funded research projects, and all garnered national, and sometimes worldwide coverage in the press.

Greenland's Ice Sheet Melting Faster - June 11 (NY Times, BBC News, UPI, Atlanta Journal Constitution) Jay Zwally (NASA/GSFC) and Waleed Abalati (NASA HQ) said that increased summer melting of Greenland's Ice Sheet is causing the ice to spread and thin.

Large Volcanic Eruptions Affect the "Greener Greenhouse" – June 10 (ScienceDaily.com) Boston University researcher Ranga Myneni said that large volcanic eruptions slow plant growth, but enhance the ability of the lands to act as a carbon sink.

Climate Change May Become Major Player in Ozone Loss – June 4 (SpaceDaily, ENS News) Drew Shindell (NASA/GISS) used model simulations to determine that climate change from greenhouse gases may affect the protective ozone layer.

NASA Developing Radar to Locate Lost Planes - June 5 (Space.com) David Imel (NASA/JPL) and David Affens (NASA/Goddard) discuss NASA's

involvement in the development of an AIRSAR for search and rescue. AIRSAR was installed on NASA's DC-8 for an April 1 simulated search and rescue mission.

Glacier Melts Will Have Global Impacts – May 30 (UPI, ENS News, Space.com) Most of the world's glaciers are melting faster than ever before, according to Jeffrey Kargel (USGS), who was part of a USGS and NASA joint assessment of glaciers.

NASA Sensors Find Pollution Hiding in the "Shadoz" - May 30 (Spaceflightnow.com, Space.com) Anne Thompson (NASA/GSFC) found that pollutants travel the globe and pile up over the Atlantic Ocean.

NASA Satellite Imagery - May 29 (ABCNews.com) NASA Archeologist Tom Sever (NASA/MSFC) discussed NASA's involvement in a National Science Foundation study of ancient footpaths in Costa Rica, for which NASA is providing satellite imagery.

Rainfall Can Predict El Niños - May 29 (UPI, SpaceDaily.com) Scott Curtis (NASA/GSFC and UMBC) and Bob Adler (NASA/GSFC) are looking at rainfall patterns around the world to predict El Niño.

Warm Polar Winter Easier on Arctic Ozone - June 3 (SpaceDaily.com, UPI) GSFC researcher, Susan Strahan found that upper level ozone levels were higher than usual because of a rare sudden warming during the early winter of 1998.

Laser 'Radar' Tracks Quakes, Climate – May 29 (UPI) Waleed Abdalati (NASA HQ) was quoted in this article about researchers using LIDAR, a ranging and location system based on light instead of radio waves, to monitor changes in geologic faults and ice sheets.

Satellites to Help Collate Fire Data, Weather Forecasts - May 28 (Scripps Howard News Service) A consortium of scientists has patched together a network of satellite images to watch fires across the entire Western Hemisphere, Jeffrey Reid (U.S. Navy) is quoted.

Mapping Standards To Help Community Flood Preparedness - May 23 (Times-Picayune) Bruce Davis (NASA/Stennis Space Center) explains remote-sensing projects at work in North Carolina, Texas, and Mexico to determine optimum flood-mapping standards.

Scientists Begin Dust-Devil Experiment – May 21 (SpaceflightNow.com) Scientists from several nations began an experiment to discover how dust devils may affect atmospheres on Earth and on Mars. John Marshall (NASA/Ames), William Farrell (NASA/GSFC), and Barry Hillard (NASA/John Glenn Research Center) were named in the story.

Changes in Rainfall Patterns Affect Plants, Carbon in U.S. – May 20 (Science, UPI, Spaceflight Now, Cosmiverse.com) Steve Running (Univ. of MT) and Ramakrishna Nemani

(Univ. of MT) found that changing rainfall patterns over much of the United States in the last century have allowed plants to grow more vigorously and absorb more carbon dioxide from the atmosphere.

Taking the Temperature of a Hurricane's Eye – May 16

(Cosmiverse.com, Universe Today) When hurricane Erin was beating up the North Atlantic last year, Jeff Halverson (NASA/GSFC) and other

NASA-funded researchers took Erin's eye temperature.

Shutdown of Airlines Aided Contrail Studies – May 11 (ScienceNews)

The September airline shutdown allowed scientists, such as Patrick Minnis (NASA/Langley) a rare glimpse into the effects of airplane contrails on climate.

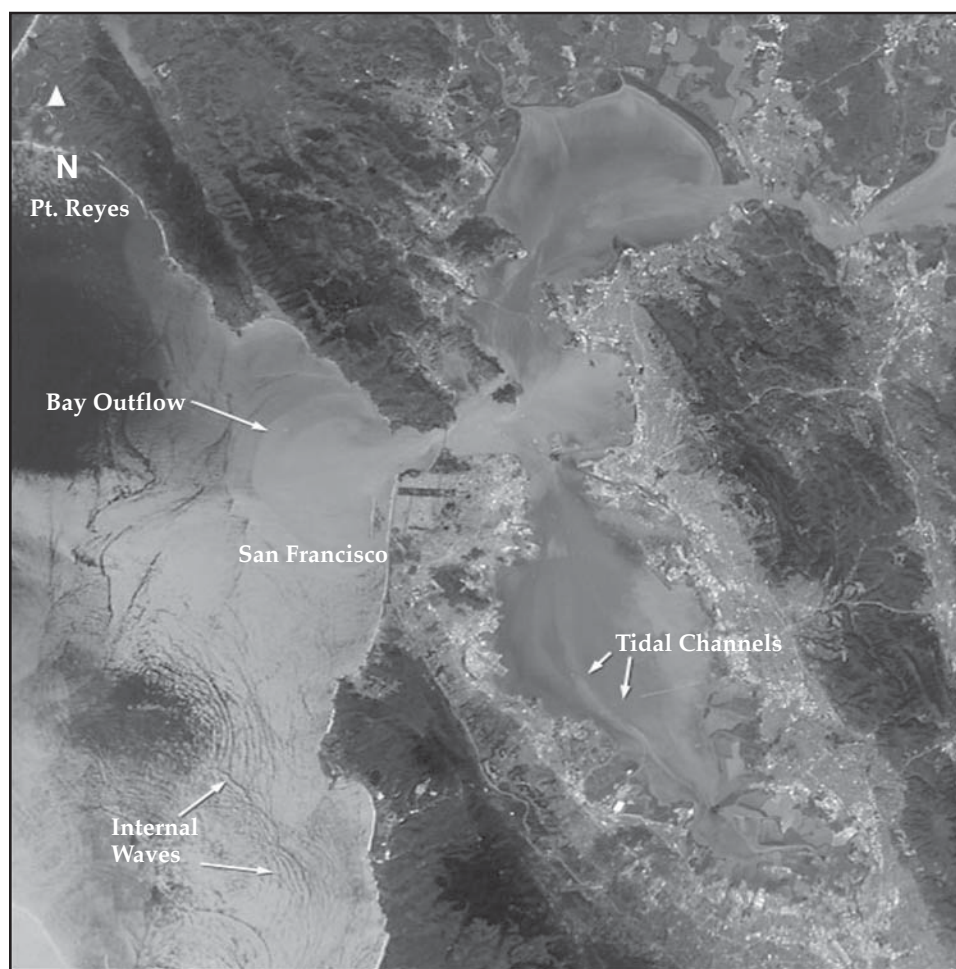
Lightning as a Predictor of Tornadoes

- May 9 (ABC World News Tonight

With Peter Jennings) Hugh Christian (NASA/MSFC) discussed research in using lightning activity to help predict tornadoes.

Pollution May Discourage Thunderclouds – May 3 (UPI, Cosmiverse.com)

Steven Sherwood (Yale University) said tiny aerosols or airborne particles of pollution may alter the size of ice crystals and increase the quantity of them in thunderclouds.



ISS IMAGE OF SAN FRANCISCO BAY AND VICINITY. Astronauts aboard the International Space Station (ISS) recently photographed the San Francisco Bay area. The gray urban footprint of San Francisco, Oakland, San Jose, and their surrounding suburbs contrast strongly with the lush hillsides. Of particular note are the Pacific Ocean water patterns that are highlighted in the sun glint. Sets of internal waves traveling east impinge on the coastline south of San Francisco. At the same time, fresher bay water flows out from the bay beneath the Golden Gate Bridge, creating a large plume traveling westward. Tidal current channels suggest the tidal flow deep in the bay. Because the ISS orbits are not synchronous with the sun, astronauts view the Earth with variable solar illumination angles. This allows them to document phenomena such as the sun reflecting differentially off surface waters in a way that outlines complicated water structures. **Image Credit:** Earth Sciences and Image Analysis Laboratory, Johnson Space Center.

Earth Science Education Program Update

- Blanche Meeson, bmeeson@see.gsfc.nasa.gov, NASA Goddard Space Flight Center
- Theresa Schwerin, Theresa_schwerin@strategies.org, IGES

Earth Tic Tac Toe — New Fun and Free

The new Earth “TicTacToe” game is now available for beta testing at earth.rice.edu/Earth_Update/module_updates/. It uses the images and movies from Earth Update as clues for the game, but it is not necessary to play an installed version of Earth Update. The developers at Rice University would like you to give it a try and tell them what you think. The rules are like “Hollywood Squares” – but you select whether you play against another person or against the computer.

If you have Earth Update installed, it will use images and movies from Earth Update as clues for the game. Just make a folder called “games” in your Earth Update folder and move the

“TicTacToe” folder into the “games” folder. That will allow the game to find the images and movies automatically.

If you don’t have Earth Update installed, just click on “TicTacToe” to play the game as is. It will ask you to browse for your Earth Update folder, but you can “cancel” if you don’t have Earth Update installed.

The “Question Editor” allows you to change the questions, to select a set of the questions to print out and use in your class as a quiz, and to make an answer key. The Earth Update project won’t be distributing the question editor with the sales version of Earth Update. After this round of beta testing, only registered e-teachers will get copies of the question editor.

U.S. Schools Compete for the 2003 GLOBE Learning Expeditions

A GLOBE Learning Expedition (GLE) will be held in June 2003 in Sibenik, Croatia. GLOBE HQ will select approximately 10 student teams to represent the United States at the GLE; each team will consist of 2-4 students accompanied by a teacher-chaperone. U.S. teams will be selected based on written presentations of student research projects. GLOBE will arrange for partial support of the winners’ costs to attend the 2003 GLE.

This international student-teacher conference will be a forum for student research teams to present the results of their research projects. It also will be an opportunity for students to experience and measure a new environment, meet other GLOBE students from around the world, and learn from each other and from GLOBE scientists. For more information, see: www.globe.gov <http://www.globe.gov>.

Science News

For the latest NASA Earth Science news, visit the NASA Earth Observatory (earthobservatory.nasa.gov) or Science@NASA (science.nasa.gov).



ESIP Federation Holds Semi-Annual Meeting in DC

The Federation of Earth Science Information Partners (ESIP) held its ninth meeting May 15-17, 2002 at the University of Maryland. Following preliminary meetings by committees, clusters, and working groups, the Assembly convened for two days of presentations and discussions from Federation members and invited guest speakers. Included among the guest speakers, were a number of representatives from NASA Headquarters including Jack Kaye. New officers were elected during the business session on the final day of the meeting. Dave Jones will serve as president of the ESIP Federation for the coming year and Jim Frew will serve as Vice President. Kudos to Dave, Jim, and all other officers.

EOS Science Calendar

July 17-19,

SORCE Science Working Group, Steamboat Springs, CO. Contact: Vanessa George, email: vanessa.george@lasp.colorado.edu, URL: lasp.colorado.edu/sorce/July02SummerMeeting.html.

July 22-24

MODIS Science Team Meeting, Greenbelt, MD. Contact: Barbara Conboy, email: bconboy@pop900.gsfc.nasa.gov, URL: modis.gsfc.nasa.gov/sci_meetings/.

July 22-26

The International Tropical Rainfall Measurement Mission (TRMM) Science Conference, Honolulu, Hawaii. Contact: Robert Adler, email: robert.adler@gsfc.nasa.gov.

September 25-27

GLAS Science Team Meeting, Boulder, CO. Contact: Bob Schutz, email: schutz@csr.utexas.edu.

Global Change Calendar

September 2-6

ISPRS Commission V Symposium, Thessaloniki, Greece. Contact: Prof. Alexandra Koussoulakou, email: kusulaku@eng.auth.gr.

September 3-6

Pan Ocean Remote Sensing Conference (PORSEC) 2002, Bali, Indonesia. Contact: Bonar Pasaribu, email: bonarpp@indosat.net.id, URL: www.porsec2001.com.

September 9-13

ISPRS Commission III Symposium 2002, Graz, Austria. Contact: Institute for Computer Graphics and Vision, email: office@icg.tugraz.ac.at, URL: www.icg.tugraz.ac.at/isprs, tel. +43 316 873-5011.

September 18-25

Joint CACGP/IGAC 002 International Symposium, "Chemistry Within the Earth System: From Regional Pollution to Global Change," Crete, Greece. Contact: Maria Kanakidou, email: mariak@chemistry.uoc.gr, URL: atlas.chemistry.uoc.gr/IGAC2002.

September 23-27

Conference on Sensors, Systems, and Next Generation Satellites VIII (RS03), an SPIE Symposium on Remote Sensing, Crete, Greece. Contact Steve Neeck, email steve.neeck@gsfc.nasa.gov, or SPIE, email: spie@spie.org.

October 14-19

COSPAR Scientific Commission A, Houston, TX. Contact Robert Ellingson, email: bobe@metosrv2.umd.edu, tel. 301-405-5386.

October 14-19

World Space Congress, Houston, TX. Contact: AIAA, email: wsc2002@aiaa.org, URL: www.aiaa.org/WSC2002/.

October 23 - 27

SPIE's Third International Asia-Pacific Environmental Remote Sensing Symposium 2002: Remote Sensing of the Atmosphere, Ocean, Environment, and Space, Hangzhou, China. URL: spie.org/Conferences/Calls/02/ae/.

October 26-28

3rd International Symposium on Sustainable Agro-environmental Systems: New Technologies and Applications, Cairo, Egypt. Contact Derya Maktav, email: dmaktav@ins.itu.edu.tr.

November 10-15

PECORA 15/Land Satellite Information IV Conference, Denver, CO. Contact: Ron Beck, email: beck@usgs.gov, URL: www.asprs.org/Pecora-ISPRS-2002/program.html.

November 18-22

WOCE and Beyond: Achievements of the World Ocean Circulation Experiment, San Antonio, TX. Contact: Maureen Reap, email: woce2002@tamu.edu, URL: www.woce2002.tamu.edu.

December 3-6

International Symposium on Resource and Environmental Monitoring, Hyderabad, India, Contact R. Nagaraja, email: nagaraja_r@nrnsa.gov.in, tel. 91-40-388-4239.

December 6-10

American Geophysical Union Fall Meeting, San Francisco, CA. Contact: E. Terry, email: eterry@agu.org, URL: www.agu.org/meetings/fm02top.html.

December 9-13

NOAA Satellite Direct Readout Conference for the Americas, Miami, Florida. Email: satinfo@noaa.gov, URL: noaasis.noaa.gov/miami02.

2003

February 9-13

American Meteorological Society Conference, Long Beach, CA. Email: amsinfo@ametsoc.org, URL: ametsoc.org/AMS/.

February 13-18

AAAS Annual Meeting, Denver, CO. URL: www.aaas.org/meetings/.

July 21-25

IGARSS 2003, Toulouse, France. Email: grss@ieee.org, URL: www.igarss03.com.

Code 900
National Aeronautics and
Space Administration

Goddard Space Flight Center
Greenbelt, Maryland 20771

Official Business
Penalty For Private Use, \$300.00

PRSRT STD
Postage and Fees Paid
National Aeronautics and
Space Administration
Permit G27

The Earth Observer

The Earth Observer is published by the EOS Project Science Office, Code 900, NASA Goddard Space Flight Center, Greenbelt, Maryland 20771, telephone (301) 614-5559, FAX (301) 614-6530, and is available on the World Wide Web at eos.nasa.gov/ or by writing to the above address. Articles, contributions to the meeting calendar, and suggestions are welcomed. Contributions to the calendars should contain location, person to contact, telephone number, and e-mail address. To subscribe to *The Earth Observer*, or to change your mailing address, please call Hannelore Parrish at (301) 867-2114, send message to hannelore_parrish@sesda.com, or write to the address above.

The Earth Observer Staff:

Executive Editor: Charlotte Griner (charlotte.griner@gsfc.nasa.gov)
Technical Editors: Bill Bandeen (bill_bandeen@sesda.com)
Tim Suttles (4suttles@bellsouth.net)
Reynold Greenstone (rennygr@earthlink.net)
Jim Closs (jim.closs@gsfc.nasa.gov)
Design and Production: Alan Ward (alan_ward@sesda.com)
Distribution: Hannelore Parrish (hannelore_parrish@sesda.com)



Printed on Recycled Paper